JOURNAL OF COMPUTATIONAL PHYSICS 59, 1–55 (1985)

Review Article

The Monte Carlo Method for the Study of Phase Transitions: A Review of Some Recent Progress

K. BINDER

Institut für Physik, Universität Mainz, D-6500 Mainz, Postfach 3980, Germany

Received September 19, 1984

For the statistical mechanics of many-body systems Monte Carlo methods have become a well-established tool. A particularly popular application is the study of statics and dynamics of phase transitions of lattice models. Here some aspects of these studies are reviewed, with a particular emphasis on problems illustrating general progress in the implementation of the method and in the analysis of the results. Finite-size effects will be given a detailed consideration, and finite-size scaling at both second- and first-order transitions will be discussed, as well as the study of inhomogeneous systems (containing interfaces or surfaces). Methods for sampling the entropy will be mentioned. Finally studies of diffusion problems and the simulation of the approach towards equilibrium in quenching experiments will be described. In the Conclusions those questions are pointed out where Monte Carlo methods still can give only rather unsatisfactory answers, such as equilibrium properties of strongly disordered systems.

1. INTRODUCTION

When the Monte Carlo method was introduced into the field of statistical thermodynamics by Metropolis, Rosenbluth and Teller [1], more than thirty years ago, a study of a phase transition was already involved: computing the equation of state of a system of hard disks, a transition from a fluid to a solid phase is observed. Subsequently the method was applied to many other phase transition problems, including those occurring in lattice systems such as the Ising model [2, 3] or classical Heisenberg model [3] of magnetism. These early studies of lattice models showed rather clearly two main limitations of the method: (i) due to the finite size of the system both the location of a phase transition and the quantitative analysis of its properties are severely hampered. In fact, statistical mechanics tells us that the occurence of phase transitions is intimately linked to the thermodynamic limit, particle number $N \to \infty$; in a finite system a phase transition in strict sense cannot occur at all—any singularities associated with the transition in the infinite system

0021-9991/85 $3.00

(jump singularities of extensive thermodynamic quantities and latent heat at first-order phase transitions; singular specific heat and order parameter susceptibility at second-order transitions) are washed out in the finite system. (ii) Due to the fact that one generates subsequent "microstates" of the system one from the other via a Markov process, these subsequent configurations are "dynamically correlated" with each other. These "dynamic correlations" increase dramatically near a phase transition, and make an extensive sampling necessary even for reaching a modest accuracy of the quantities of interest. Of course, these "dynamic correlations" need not at all be related to the intrinsic dynamical behavior the considered model might have; the Monte Carlo method can be viewed as a numerical realization of a master equation, which sometimes—but by no means always—is a reasonable representation of the dynamics of the considered model [4]. While this aspect of the method allows one to study the dynamics of some models of nonequilibrium statistical thermodynamics, it often prevents one from reaching the desired accuracy.

These limitations are by no means restricted to lattice systems; in fact, the recent controversy about whether simulations of 2-dimensional melting [5] exhibit a first-order transition or two second-order transitions with the so-called hexatic phase in between, as suggested by some theoretical treatments [6], shows that even the problem studied already by Metropolis *et al.* [1] is not yet clarified. But this review will restrict attention to lattice systems, because only in this area have the above two limitations been considered in great detail; in fact, the quantitative study of finite-size rounding of singularities at phase transitions has become a computational tool for an analysis of the transition of the infinite system. Although there are many topics in the simulation of classical fluids (for reviews of the truly abundant literature in this field see [7–11]), where finite-size effects play little rôle, the present considerations should apply to phase transitions in such off-lattice systems as well (e.g., gas-liquid transition, unmixing in binary fluids, melting, solid-solid phase transformations, superionic conductors, etc.).

The main theme of this article hence is the understanding of finite-size effects and finite "observation-time" limitations, or expressed from a somewhat different point of view, an analysis of the *relevant length scales* and *relevant "time" scales* for a given problem. Consideration of these scales is absolutely essential for the *judgement of the computational needs* of a given problem: while in the extreme case some problems are even simple enough so that they even can be treated on minicomputers [12, 13], for other problems one needs to resort to extremely high-speed special purpose processors [14–17]—and maybe even these machines are yet too limited in their computational power to answer certain questions, as we shall discuss below. Fortunately, there exists a large class of problems which can be treated in an effective way on recent high-speed general purpose computers, as they are typically available for scientific use.

An area which has seen remarkable recent progress but which is not covered in the present article is the Monte Carlo simulation of quantum-mechanical lattice systems, such as the quantum Heisenberg model and related models (e.g., [18–26]).

Some aspects of the present review, such as finite-size effects and finite-size scaling, are also useful for work on quantum problems, however (see, e.g., [24]). Another disclaimer is in order at the end of this introduction: no attempt is made to give a complete list of various applications (extensive reviews can be found in [27, 28]). In addition, we shall not discuss the explicit implication of computer codes and special techniques which can save memory and speed up a program, such as multi-spin-coding (for descriptions of this technique see [29–34]) or the "n-fold way" which is useful for simulations at very low temperatures (see [35–37]). Thus the present article does not discuss how Monte Carlo programs are written, but rather how results obtained with such programs are appropriately analyzed and interpreted.

In Section 2, we shall briefly review the general theoretical background on the Monte Carlo method (more detailed accounts are found in [7, 8, 27, 28], for instance). Section 3 will be devoted to a discussion of finite size effects in terms of finite size scaling theories, which will be exposed both for second-order and for first-order transitions. Other types of finite-size effects will also be mentioned briefly. Section 4 then discusses some aspects pertinent to the simulation of systems containing surfaces or interfaces, and related questions such as estimation of the interfacial free energy. The problem of sampling the bulk free energy or entropy is discussed in Section 5.

The last two sections of this article deal with applications to dynamic properties: as an example for the study of the dynamics of fluctuations in equilibrium states, we shall discuss studies of diffusion in lattice gases, where one wishes to determine both self-diffusion constants and collective diffusion constants, in Section 6. As an example for the study of the dynamics of far-from-equilibrium systems, Section 7 discusses the kinetics of ordering and domain formation in systems undergoing order–disorder phase transitions. Finally Section 8 summarizes our conclusions and also discusses some questions where Monte Carlo methods still can give only very limited results, such as the random-field Ising problem or the question whether short-range spin glasses in three dimensions have a phase transition at nonzero temperature.

Although this article emphasizes Monte Carlo studies of phase transitions, it will not present an exposition of Monte Carlo renormalization group techniques: these very useful techniques have recently been brilliantly reviewed elsewhere [38]; in addition, an adequate description of them requires some background about the renormalization group in general, which is beyond the scope of the present article.

2. Computation of Static Averages by Importance Sampling Monte Carlo Methods

We consider a system of N particles which can exist at the sites i of a d-dimensional lattice of linear dimension L at a temperature T. Other intensive thermodynamic variables may be specified in addition: e.g., for magnetic systems we

may have an applied magnetic field H or a staggered field H_s which has a different sign at different sublattices, or local fields which act at certain sites only, or on the surfaces of the system when we deal with the simulation of a system with (some) free boundaries. This point already illustrates one advantage of the Monte Carlo "computer experiment" as compared to a real laboratory experiment: one may study the effect of "fields" which may have a significance in theoretical treatments, but are not accessible in the laboratory.

Each of the particles now is described by a set of dynamical variables $\{\alpha_i\}$ representing its degrees of freedom. In order to give some specific examples we mention some of the most commonly studied models, which also will serve later in this article to illustrate the points made there: the lattice gas model is characterized by an occupation variable c_i which just may take two values only, $c_i = 1$ if the lattice site i is taken by a particle, and $c_i = 0$ if it is empty. Double occupancy of lattice sites is forbidden. Thus a typical Hamiltonian $\mathscr{H}_{LG}$ for such a model is

$$\mathscr{H}_{LG} = -\varepsilon \sum_i c_i - \sum \phi_{ij} c_i c_j - \sum \phi_{ijk} c_i c_j c_k - \cdots, \tag{1}$$

where ε is a binding energy to the lattice site, ϕ_{ij} a pairwise interaction parameter, ϕ_{ijk} a triplet interaction parameter, etc. This example already leads us to discuss the freedom of the choice in the statistical ensemble: the model as it stands is specified by the thermodynamic variables volume $V = L^d$ (for simplicity we shall take the lattice as cubic and measure lengths in units of the lattice spacing; but the generalization to other lattices should be obvious), the particle number N, and the temperature T. This is the canonical ensemble. Instead we might like to work in the grand-canonical ensemble, where instead of N the conjugate thermodynamic variable, the chemical potential μ, is specified; or we might work in the microcanonical ensemble, where N is kept but T is replaced by the internal energy of the system (for recent studies applying this latter ensemble see [39]). Of course, it is well known that in the thermodynamic limit $N \to \infty$, these various ensembles yield equivalent results. This is not true for finite systems, however, some finite size effects are different in different ensembles [40].

Thus the question arises, which is the most appropriate ensemble to choose for a Monte Carlo calculation. Of course, there is no general answer to this question. Since the fact that any extensive thermodynamic variable is kept constant implies that long-wave length fluctuations of the associated density of that variable are slowly relaxing, the approach towards equilibrium typically is quickest in the grand-canonical ensemble containing intensive thermodynamic variables as its parameters only.

However, the choice of the canonical ensemble may be more convenient when for some reason one wishes to strictly suppress the fluctuation of the particle number, $\langle N^2 \rangle_T - \langle N \rangle_T^2$, which would be present in the grand-canonical ensemble. The choice of the canonical ensemble is also necessary when we wish to study coexistence between two different phases: in a finite system, the interfacial con-

tribution to the energy of such states is important [41], and therefore in the equivalent grand-canonical simulation such states occur with very low probability only [42]. We shall return to such questions in Section 4. At this point, we only mention that sometimes it even is advantageous to *change the ensemble* during the simulation itself: for the simulation of diffusion in lattice gases (see Sect. 6 and [43]) one may first produce an equilibrium state at the desired temperature by a grand-canonical simulation, and use then configurations typical for that state as the initial configuration for the run simulating the diffusion process (for which necessarily the particle number must be kept constant). Another situation where only a canonical ensemble is applicable is encountered when the simulated objects are large and take many lattice sites: this happens for instance in the simulation of dense polymer systems, where each polymer chain is represented by a self-avoiding walk on the lattice.

The other models which will frequently be mentioned in this article are models of magnetic systems, where a spin variable is associated to each lattice site. If this variable can take just two values, $s_i = \pm 1$, we get the Ising model of magnetism

$$\mathscr{H}_I = -\sum_{i \neq j} J_{ij} S_i S_j - H \sum_i S_i, \tag{2}$$

J_{ij} being the exchange energy between spins at sites i and j, and H is a uniform magnetic field. As is well known, this model is isomorphic to the lattice gas model with pairwise interactions (see, e.g., [44]). If the spins are n-component (classical) unit vectors $\mathbf{s}_i = (s_i^1, s_i^2, ..., s_i^n)$, one gets the n-vector model

$$\mathscr{H} = -\sum_{i \neq j} J_{ij} \mathbf{S}_i \cdot \mathbf{S}_j - H \sum_i S_i^n; \tag{3}$$

for $n = 2$ this model also is called XY model, for $n = 3$, Heisenberg model. Of course, this list of lattice models by no means is exhaustive (for lattice models of molecular crystals or liquid crystals the local degree of freedom is neither a scalar nor a vector, but rather a tensor of second rank, etc.); we have here just introduced those models which later on will be used as examples to illustrate more general points.

The set of dynamical variables of the chosen model then defines the phase space, which contributes to the thermal averages. Denoting a phase space point as $\mathbf{X} = \{\alpha_1, \alpha_2, ..., \alpha_N\}$, the average of an observable $A(\mathbf{X})$ in the canonical ensemble takes the well-known form

$$\langle A \rangle = \frac{1}{Z} \int_\Omega d\mathbf{X}\, A(\mathbf{X}) \exp[-\mathscr{H}(\mathbf{X})/k_B T], \tag{4a}$$

$$Z = \int_\Omega d\mathbf{X} \exp[-\mathscr{H}(\mathbf{X})/k_B T], \tag{4b}$$

where Ω denotes the volume of phase space, and k_B denotes Boltzmann's constant.

In cases where the α_i can take discrete variables only, the integrals stand symbolically for the respective sums.

The basic idea of the Monte Carlo method now is to calculate the phase space integrals in Eq. (4) numerically, by a sampling technique where one chooses M points $\mathbf{X}_\gamma$ at random in order to approximate these integrals by corresponding sums over these points. It is well known, however, that the probability distribution $p(\mathbf{X}) = (1/Z) \exp[-\mathcal{H}(\mathbf{X})/k_B T]$ has a very sharp peak in that region of phase space where all extensive variables $A(\mathbf{X})$ are close to their averages values $\langle A \rangle$: this peak may be approximated [45] by a gaussian centered at $\langle A \rangle$, with a relative halfwidth of order $1/\sqrt{N}$ only. Hence for a practical useful method one cannot sample the phase space uniformly ("simple random sampling" method [27, 28]), but the points $\mathbf{X}_\gamma$ must be chosen preferentially from the important region of phase space, the vicinity of the peak of this probability distribution. This goal is achieved by the importance sampling Monte Carlo method first introduced by Metropolis *et al.* [1]. Starting from some initial configuration $\mathbf{X}_1$, one constructs a Markov process which is defined in terms of a transition probability $W(\mathbf{X}_\gamma \to \mathbf{X}'_\gamma)$, and hence one creates a "random walk" through phase space. The idea of that method is to choose $W(\mathbf{X} \to \mathbf{X}')$ such that the probability with which a point $\mathbf{X}$ is chosen in this process converges towards the canonical probability $P_{\text{eq}}(\mathbf{X}) = (1/Z) \exp[-\mathcal{H}(\mathbf{X})/k_B T]$ in the limit $M \to \infty$. A condition sufficient to ensure this convergence is the principle of detailed balance,

$$P_{\text{eq}}(\mathbf{X})\, W(\mathbf{X} \to \mathbf{X}') = P_{\text{eq}}(\mathbf{X}')\, W(\mathbf{X}' \to \mathbf{X}). \tag{5}$$

Less restrictive conditions for the transition probability are considered in [2, 7, 46, 47], but will not be discussed here. For a justification that Eq. (5) actually yields this desired convergence we also refer to the literature [1, 2, 7, 8, 27, 28, 46, 47]. Here we only note that in this importance sampling technique the average Eq. (4) is estimated in terms of a simple arithmetic average,

$$\bar{A} = 1/(M - M_0) \sum_{\gamma = M_0 + 1}^{M} A(\mathbf{X}_\gamma). \tag{6}$$

Here we have already anticipated that it is advantageous to eliminate the residual influence of the initial configuration $\mathbf{X}_1$ by eliminating an appropriate number M_0 of states from the average.

What is now meant in practice by the transition $\mathbf{X} \to \mathbf{X}'$? Again there is no general answer to this question, the choice of the process may depend both on the model under consideration, and the purpose of the simulation. Since Eq. (5) implies that

$$\frac{W(\mathbf{X} \to \mathbf{X}')}{W(\mathbf{X}' \to \mathbf{X})} = \exp(-\delta\mathcal{H}/k_B T), \tag{7}$$

where $\delta\mathscr{H}$ is the energy change brought about by the move from $\mathbf{X}$ to $\mathbf{X}'$, it clearly is necessary to consider small changes of the state $\mathbf{X}$ only: otherwise the absolute value of the energy change $|\delta\mathscr{H}|$ would be rather large and either $W(\mathbf{X}\to\mathbf{X}')$ or $W(\mathbf{X}'\to\mathbf{X})$ would be extremely small. Then it would be almost always forbidden to actually carry out the corresponding move, and the procedure would be poorly convergent. Thus, in the lattice gas model at constant particle number, a transition $\mathbf{X}\to\mathbf{X}'$ consists of moving just one particle to a (randomly chosen) neighboring site, rather than moving a larger number of particles simultaneously, although in principle that would be possible. In the lattice gas model at constant chemical potential, one removes (or adds) just one particle at a time, which is the isomorphic process to single spin-flips in the Ising model. One has more freedom in choosing the move $\mathbf{X}\to\mathbf{X}'$ if the local degrees of freedom are continuous variables, of course. For instance, in the classical XY model the local degree of freedom is the angle φ_i between spin direction at site i and the x-axis. Then the transition $\mathbf{X}\to\mathbf{X}'$ may consist of a change of φ_i to a value $\varphi_i'=\varphi_i+\eta\,\Delta\varphi$, where η is a random number uniformly distributed between -1 and $+1$. The step parameter $\Delta\varphi$ is arbitrary, but is conveniently chosen such that, on the average, the transition probability is one half (or nearly so).

Another arbitrariness concerns the order in which the particles are selected for considering a move. Often one chooses to select them in the order of their labels (in a simulation of a fluid or lattice gas at constant particle number) or to go in a regular way through the lattice (in the case of spin models, for instance). An often used alternative is to go at random through the lattice sites (or particle numbers, respectively). The latter procedure is somewhat more time-consuming, but it is a more faithful representation of a dynamic time evolution of the model described by a master equation (see Sect. 6).

Finally we have to discuss the arbitrariness in the choice of the transition probability $W(\mathbf{X}\to\mathbf{X}')$ itself. The choice originally supported by Metropolis *et al.* [1] is

$$\begin{aligned} W(\mathbf{X}\to\mathbf{X}') &= \exp(-\delta\mathscr{H}/k_B T) \qquad \text{if} \quad \delta\mathscr{H}>0, \\ &= 1 \qquad\qquad\qquad\quad \text{else.} \end{aligned} \tag{8}$$

An alternative choice, which is that commonly used in the context of kinetic Ising models [48], is

$$W(\mathbf{X}\to\mathbf{X}') = \exp(-\delta\mathscr{H}/k_B T)/[1+\exp(-\delta\mathscr{H}/k_B T)]. \tag{9}$$

In an Ising model, the choice Eq. (9) is identical to the so-called "heatbath"-method [49]: in this method one assigns the new value α_i' of the local degree of freedom in the move from $\mathbf{X}$ to $\mathbf{X}'$ irrespective of what the old value α_i was. One thereby considers the local energy $\mathscr{H}_i(\alpha_i')$ and chooses the state α_i with probability $\exp[-\mathscr{H}_i(\alpha_i')/k_B T]/\sum_{\{\alpha_i''\}}\exp[-\mathscr{H}_i(\alpha_i'')/k_B T]$.

The practical efficiency of the Metropolis method and the heatbath method have been compared both for the case of kinetic Ising models [50] and for the case of lattice gauge theories [51]; in these cases the efficiency was roughly comparable.

It remains to outline the algorithm which realizes the Markov chain with a chosen transition probability $W(\mathbf{X} \to \mathbf{X}')$. What is done at each step of the procedure is to perform a *trial move* $\alpha_i \to \alpha_i'$, compute $W(\mathbf{X} \to \mathbf{X}')$ for this trial move and compare it with a random number η, which is uniformly distributed in the interval $0 < \eta < 1$. If $W < \eta$ the trial move is rejected, and the old state (with α_i) is counted once more in the average, Eq. (6). Then another trial is made. If $W > \eta$, on the other hand, the trial move is accepted and the new configuration thus generated is taken into account in the average, Eq. (6). It serves then also as a starting point of the next step.

Since subsequent states $\mathbf{X}_\gamma$ in this Markov chain differ by the coordinate α_i of one particle only (if they differ at all), they are highly correlated. Therefore it is not straightforward to estimate the error of the average, Eq. (6). Let us assume for the moment that after n steps these correlations have died out. Then we may estimate the statistical error δA of the estimate $\bar{A}$ from the standard formula.

$$\overline{(\delta A)^2} = \frac{1}{m(m-1)} \sum_{\mu=\mu_0}^{m+\mu_0-1} [A(\mathbf{X}_\mu) - \bar{A}]^2, \qquad m \gg 1, \tag{10}$$

where the integers μ_0, μ, m are defined such that $m = (M - M_0)/n$ and μ_0 labels the state $\gamma = M_0 + 1$ {cf., Eq. (6)}, $\mu = \mu_0 + 1$ labels the state $\gamma = M_0 + 1 + n$, etc. Then also $\bar{A}$ for consistency should be taken as $\bar{A} = (1/m) \sum_{\mu=\mu_0}^{m+\mu_0-1} A(\mathbf{X}_\mu)$.

It is not always easy to estimate the number of configurations M_0 after which the correlation to the initial state $\mathbf{X}$, which typically is a state far from equilibrium, has died out, nor is it easy to estimate n. A formal answer to this problem can be given in terms of relaxation times of the associated master equation describing the Monte Carlo process [4, 36, 47], see Section 6.

A final comment emerges when we compare the canonical average, Eq. (4), with our estimate $\bar{A}$, Eq. (6): While the normalization factor $1/Z$ in Eq. (4a) yields free energy F and entropy S via the standard thermodynamic relations

$$F = -k_B T \ln Z, \qquad S = (U - F)/T, \tag{11}$$

U being the internal energy, the normalization factor in Eq. (6) is simply the number of configurations sampled. While U can straightforwardly be obtained by an average of the Hamiltonian itself, $U = \langle \mathscr{H} \rangle \approx \bar{\mathscr{H}}$, the information on F and hence S is lost. We return to this problem in Section 5.

3. Finite Size Effects and Finite Size Scaling

As the simplest example of a system undergoing a second-order phase transition, we consider the transition of the Ising model from a paramagnetic state above the

critical temperature T_c to a state with nonzero "spontaneous magnetization" ($\pm|M_{sp}|$ for zero applied field H) below T_c. It is well known, of course, that this spontaneous symmetry breaking can occur in the thermodynamic limit only: for a finite system, there is always a nonzero probability that the system may pass from a state near $+|M_{sp}|$ to a state near $-|M_{sp}|$, as well as in the opposite direction, and therefore we have for the magnetization M for all (nonzero) temperatures

$$M(T, H=0)=\frac{1}{N}\sum_{i=1}^{N}\langle S_i\rangle_{T,H=0}=0, \tag{12}$$

irrespective of the value of N. In fact, the correct procedure for defining the order parameter M_{sp} is to consider $M(T, H)$ in nonzero field, taking first the thermodynamic limit $N\to\infty$, and then letting H tend to zero,

$$M_{sp}=\lim_{H\to 0}\lim_{N\to\infty} M(T, H). \tag{13}$$

Of course, it would be rather tedious to try this double limiting procedure with results from Monte Carlo calculations, and hence this is done only for exceptional cases (e.g., [52]). In practical calculations for Ising systems below T_c but not too close to the critical point, one finds that a magnetization $+M$ (or $-M$, respectively, depending on the initial condition) is sufficiently metastable for long observation times, and hence one can obtain estimates with a reasonable accuracy [50]. However, even above T_c a small magnetization typically will be found due to fluctuations, which in a finite system observed over a finite "time" have not completely averaged to zero; rather one will find a value $\pm\delta M$, where δM depends on both the size of the system and the "time" (length of the simulation run). Similarly, below T_c the magnetization will fluctuate in a regime $\pm(M\pm\delta M)$, and one cannot make δM arbitrarily small by making the "time" larger and larger: if the time becomes of the order of the "ergodic time," which is the "time" needed to observe transitions from $+M$ to $-M$ or vice versa, one would start averaging the magnetization to zero. This situation becomes particularly cumbersome near the critical point, where M itself strongly decreases, while the fluctuations δM increase until they ultimately become comparable with M itself.

To avoid these problems, one often only relies on observing the root mean square order parameter [3],

$$M_{rms}=\sqrt{\langle M^2\rangle_T}=\sqrt{\left\langle\left(\sum_{i=1}^{N} S_i/N\right)^2\right\rangle_T}=\sqrt{\sum_{i=1}^{N}\sum_{j=1}^{N}\langle S_iS_j\rangle_T/N}. \tag{14}$$

In particular, this has to be done in isotropic spin systems where one has a vector order parameter $\mathbf{M}_{sp}$, whose orientation is not even metastable but rather one observes a sort of "rotational diffusion" of the unit vector along $\mathbf{M}_{sp}$ [53]. Of course, the trouble with the definition Eq. (14) is that in a finite system it is nonzero at all temperatures—even at infinite temperature, where $\langle S_iS_j\rangle=\delta_{ij}$, one still

obtains $M_{\rm rms} = 1/\sqrt{N}$ [3]. At finite temperatures above T_c, where the correlations $\langle S_i S_j \rangle_T$ may be slowly decaying, $M_{\rm rms}$ even is much larger. If we restrict ourselves to periodic boundary conditions (for a discussion of various boundary conditions see, e.g., [36]), $\langle S_i S_j \rangle_T$ is translationally invariant and hence $M_{\rm rms} = \sqrt{\sum_{i=1}^{N} \langle S_i S_j \rangle_T / N}$. It is interesting to consider this expression at the critical point itself [54]. Assuming that the correlation function behaves there qualitatively in the same way as in the infinite system (for distances r between i and j less than $L/2$),

$$\langle S_i S_j \rangle_T \propto r^{-(d-2+\eta)}, \tag{15}$$

where η is the critical exponent describing the decay of correlations at criticality (see, e.g., [55]), one obtains [54]

$$\sum_{i=1}^{N} \langle S_i S_j \rangle_T \propto \int_0^{L/2} r^{d-1}\, dr \langle S_i S_j \rangle_T \propto \int_0^{L/2} r^{1-\eta}\, dr \propto L^{2-\eta}. \tag{16}$$

This estimate yields for the size-dependence of the root mean square magnetization [54]

$$M_{\rm rms} \propto \sqrt{L^{-(d-2+\eta)}} \propto L^{-\beta/\nu} = N^{-\beta/d\nu} = N^{-1/(\delta+1)}, \tag{17}$$

where we have used the scaling laws involving the exponents β, ν, δ of order parameter, correlation length, and critical isotherm [55], $(d-2+\eta)\nu = 2\beta$, $d\nu = \beta(\delta+1)$. In an Ising model, $\delta = 3$ for dimensionalities $d \geqslant 4$, while $\delta \approx 5$ for $d=3$ and $\delta = 15$ for $d=2$ [55, 56]. Thus one finds that the critical behavior of the considered model shows up in the finite size effects, and hence it is difficult to extrapolate Monte Carlo results taken for finite lattice sizes to the thermodynamic limit.

This problem of finite size effects at phase transitions has found widespread attention in the literature [54, 57–79]. Finite size effects at second-order phase transitions are described in terms of the Fisher [59] finite-size scaling theory. This theory has been checked by Monte Carlo calculations for various models and found to give a satisfactory description even for rather small systems already [61–64]. This theory now has become a powerful tool for the study of critical phenomena [65].

We expose this theory here emphasizing a description in terms of the probability distribution of the order parameter (in an Ising ferromagnet the magnetization) [66]. For temperatures T above T_c and linear dimensions L much larger than the correlation length ξ of order parameter fluctuations this distribution should be a gaussian,

$$P_L(s) = L^{d/2}(2\pi k_B T \chi_{(L)})^{-1/2} \exp[-s^2 L^d/(2k_B T \chi_{(L)})], \qquad T > T_c, H = 0. \tag{18}$$

The "susceptibility" $\chi_{(L)}$ defined in Eq. (18) from the halfwidth of the distribution should smoothly tend towards the susceptibility χ of the infinite system as $L \to \infty$. For $T < T_c$ but again $L \gg \xi$ the distribution is peaked at values $\pm M_L$ near $\pm M_{sp}$; near those peaks again a description in terms of gaussians is appropriate (while a different behavior applies near $s = 0$ [66, 42]),

$$P_L(s) = \frac{L^{d/2}}{(2\pi k_B T \chi_{(L)})^{1/2}} \left\{ \frac{1}{2} \exp\left[- \frac{(s - M_L)^2 L^d}{2 k_B T \chi_{(L)}} \right] + \frac{1}{2} \exp\left[- \frac{(s + M_L)^2 L^d}{2 k_B T \chi_{(L)}} \right] \right\}, \qquad T < T_c, \; H = 0. \tag{19}$$

The small value of $P_L(s \approx 0)$ measures the probability that the system moves from the region near $+M_L$ to the region near $-M_L$; since the observation time needed to see such transitions increases with L as $P_L(s = M_L)/P_L(s = 0)$, it is clear that for large enough L one does not observe such transitions for physically reasonable observation times. Hence one does then not sample the full symmetric distribution, Eq. (19) for which $\langle s \rangle_L = \int_{-\infty}^{+\infty} s P_L(s)\, ds = 0$, but rather only one half of it, e.g., for s positive

$$\langle s \rangle'_L = \int_0^\infty s P_L(s)\, ds \Big/ \int_0^\infty P_L(s)\, ds = \langle |s| \rangle_L. \tag{20}$$

When Eq. (19) is an accurate description of the actual distribution, the restricted average $\langle s \rangle'_L$ coincides with the peak position M_L. From this consideration it is obvious that M_{sp} can be estimated from any of the following limits

$$\lim_{L \to \infty} M_L = \lim_{L \to \infty} \langle s \rangle'_L = \lim_{L \to \infty} \langle |s| \rangle_L = \lim_{L \to \infty} \sqrt{\langle s^2 \rangle_L} = M_{sp}. \tag{21}$$

Of course, these relations are more convenient than Eq. (13). Similarly the susceptibility can be estimated both from the fluctuation–dissipation relation (relating it to magnetization fluctuations), and the halfwidths, Δs or heights of the peaks:

$$\lim_{L \to \infty} \frac{\langle s^2 \rangle L^d}{k_B T} = \lim_{L \to \infty} \frac{P_L^{-2}(0) L^d}{2\pi k_B T} = \lim_{L \to \infty} \frac{(\Delta s)^2 L^d}{8 k_B T \ln 2} = \chi, \qquad T > T_c, \tag{22}$$

or

$$\lim_{L \to \infty} \frac{1}{k_B T} (\langle s^2 \rangle - \langle |s| \rangle^2) L^d = \lim_{L \to \infty} \frac{P_L^{-2}(M_L) L^d}{8\pi k_B T} = \lim_{L \to \infty} \frac{(\Delta s)^2 L^d}{8 k_B T \ln 2} = \chi, \qquad T < T_c. \tag{23}$$

Since often L is not very much larger than ξ and then $P_L(s)$ is described by Eqs. (18), (19) only approximately, the quantities M_L, $\langle |s| \rangle_L$, $\langle s^2 \rangle_L^{1/2}$ may deviate distinctly from each other (and from M_{sp}); similar deviations occur for the various quantities in Eqs. (22), (23) relating to the susceptibility. It is then useful to perform

several of the extrapolations suggested by Eqs. (21)–(23) simultaneously. An example is given in Fig. 1 [79], where the various system sizes simply were obtained by dividing one large system (of size 24^3) into subsystems of sizes 2^3, 3^3, 4^3, 6^3, and 8^3. Such a division into subsystems [73] is very convenient: one obtains information on size effects in a single run! A study of subsystems is also useful when one performs calculations where an extensive thermodynamic variable rather than the conjugate intensive quantity is kept constant as an independent variable. Here this would be the magnetization s: one would then no longer be able to estimate χ from any of the relations Eqs. (22), (23) for the total system. Since in subsystems s is not fixed, however, Eqs. (22), (23) then could still be applied. This point might be useful for Monte Carlo calculations of fluids and fluid mixtures, where typically the particle number (and the concentration, respectively) are held fixed. The corresponding response functions analogous to χ for these systems could then be found from the distribution functions of density (or concentration, respectively) in subsystems.

Equations (18), (19) should hold for $L \gg \xi$. However, in a practical calculation ξ often is not known, and it is quite cumbersome to calculate it from studying the decay of the correlation function $\langle S_i S_j \rangle$ wth distance. It is much easier to check the gaussian nature of the distribution by calculating the fourth-order cumulant U_L [66] (or the equivalent quantity $g_L = -3U_L$ which is called the "renormalized coupling constant" [71, 73, 16])

$$U_L = 1 - \frac{\langle s^4 \rangle_L}{3\langle s^2 \rangle_L^2}. \tag{24}$$

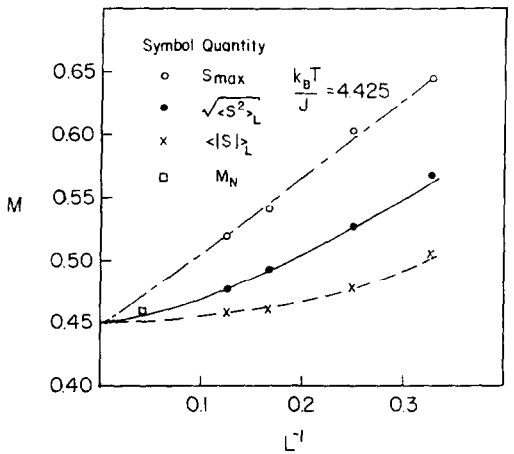

FIG. 1. Estimates of the spontaneous magnetization of the 3-dimensional Ising model with nearest-neighbor interaction on the simple cubic lattice at a temperature $k_B T/J = 4.425$ below criticality ($k_B T_c \approx 4.51$), as obtained from extrapolating the size dependence of the maximum (s_{max}) and the moments $\langle s^2 \rangle_L$ and $\langle |s| \rangle_L$ towards $L^{-1} \to 0$, for subsystems of a system of linear dimension 24 (estimate of the magnetization of the total system is denoted as M_N). From [79].

For $T > T_c$ and $L \gg \xi$, U_L decreases towards zero as $U_L \propto L^{-d}$ [66]. For $T < T_c$ and $L \gg \xi$, U_L tends to $U_\infty = \frac{2}{3}$. For $L \ll \xi$, on the other hand, U_L varies only weakly with temperature and linear dimension, it stays close to the (universal but nontrivial) "fixed-point"-value U^*.

This behavior of the cumulant makes it rather suitable for obtaining estimates of T_c itself which are not biased by any assumptions about critical exponents [66]. One may plot U_L and $U_{L'}$ with $L' = bL$, $b > 1$, versus temperature and may estimate T_c from the temperature where these curves intersect. Extrapolation of these intersection points to $L \to \infty$ yields an estimate for T_c in the 3-dimensional Ising model which is competitive in accuracy with the most extensive series expansion estimates available [16], $J/k_B T_c = 0.221650(\pm 5)$.

Figure 2 presents two nontrivial examples where this method was applied: in part A, U'_L is plotted vs U_L for the 2-dimensional XY model with and without cubic anisotropy [77]. Without anisotropy this system undergoes a Kosterlitz–Thouless transition [80] to a state without order parameter, but a power-law decay of correlation throughout the "ordered" phase. There the exponent η changes gradually with temperature. Thus T_c can be viewed as the endpoint of a line of critical points. Plotting U'_L as a function of U_L, the curve $U'_L(U_L)$ should just coincide with the diagonal in this regime, and this behavior is indeed found (Fig. 2A). If the fourfold anisotropy is added, on the other hand, an ordinary ordered phase is restored [81a] since then $U'_L > U_L$ in the ordered phase, T_c is found from the intersection of the curve U'_L (U_L) with the diagonal. Thus it is evident that a study of this "renormalized coupling constant" by Monte Carlo methods can reveal subtle

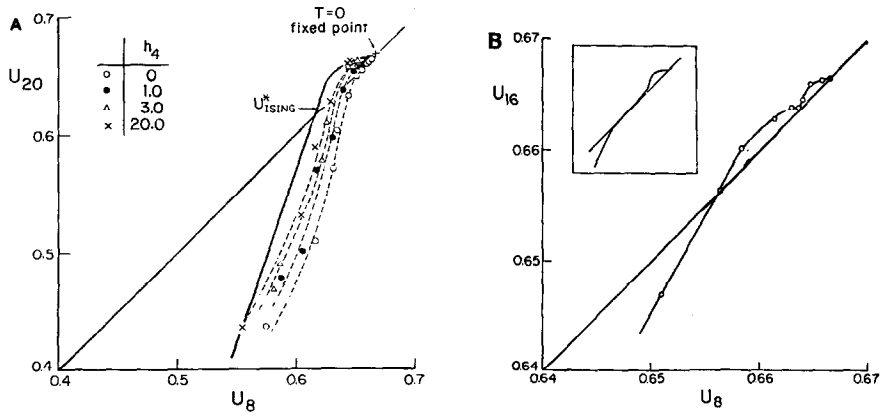

FIG. 2. (A) Cumulant U_{20} plotted vs U_8 for the 2-dimensional nearest-neighbor Ising model (full curve) and the 2-dimensional XY model where a term $-h_4 \sum[(S_i^x)^4 + (S_i^y)^4]$ has been added. Several choices of the symmetry-breaking field h_4 are shown. From [77]. (B) Cumulant U_{16} plotted vs U_8 for the 2-dimensional ferromagnetic 6-state vector Potts model [Eq. (25)]. Temperature $k_B T/J$ is a parameter of the curve. Note that two nontrivial phase transitions occur where the curve intersects (or touches, respectively) the diagonal with $U_{L'} = U_L = U^* < \frac{2}{3}$. Insert shows the expected behavior when the phase at intermediate temperature is Kosterlitz–Thouless-like. From [78].

questions about phase transitions, at least in favorable cases. Related ideas of Monte Carlo renormalization have also been applied to the square XY model by Miyashita [81b]. It must be emphasized at this point that not always can one infer straightforwardly the phase structure of the infinite system from such studies of very small systems. As an example, Fig. 2B presents the cumulant plot for the 6-state vector Potts model [81a], whose Hamiltonian is

$$\mathcal{H} = -J \sum_{\langle i,j \rangle} \cos\left[\frac{2\pi}{q}(p_i - p_j)\right], \qquad p_i, p_j = 1, 2, \ldots, q. \tag{25}$$

($q = 6$ in our case.) This model should undergo two transitions [81]: at T_2 it should have a Kosterlitz–Thouless transition to a phase with powerlaw decay of correlations, while at $T_1 < T_2$ a transition to a state with conventional long-range order should occur. The numerical data [78], Fig. 2B, do indicate two successive transitions, but the phase for $T_1 < T < T_2$ has the property $U_{L'} > U_L$ rather than the expected behavior $U_{L'} = U_L$ (as indicated in the insert). Probably in this case the lattice sizes are too small to allow for definitive conclusions about the nature of the phases. But even in this case the method seems capable of locating the critical points even more accurately than a Monte Carlo renormalization group method [82a].

Equations (18), (19) only apply in the regime where $L \gg \xi$. The behavior for $L \lesssim \xi$ can be understood by the finite-size scaling theory [59] which we formulate here also for the distribution function $P_L(s)$ [66]. The key idea is that $P_L(s) = f(L, \xi, s)$ does not depend separately on the three variables L, s, and ξ—which expresses the temperature-dependence via $\xi \propto |1 - T/T_c|^{-\nu}$—but only two combinations L/ξ, $s\xi^{\beta/\nu}$ should enter (apart from a power-law prefactor which trivially ensures the normalization $\int_{-\infty}^{+\infty} ds\, P_L(s) = 1$),

$$P_L(s) = f(L, \xi, s) = \xi^{\beta/\nu} P(L/\xi, s\xi^{\beta/\nu}). \tag{26}$$

This "ansatz" is analogous to the scaling assumption for the singular part of the free energy [55], $s\xi^{\beta/\nu}$ being the analog of $M\xi^{\beta/\nu}$,

$$F_{\text{sing}}(T, M) = \xi^{-(2-\alpha)/\nu} \tilde{f}(M\xi^{\beta/\nu}), \tag{27}$$

where α is the specific heat exponent and $\tilde{f}$ the appropriate scaling function. The scaling function P for $P_L(s)$ contains the additional variable L/ξ which expresses the idea that the *linear dimension L should scale with the correlation length* ξ. We now rewrite Eq. (26) using $sL^{\beta/\nu}$ as a variable instead of $s\xi^{\beta/\nu}$ (the function P then changes to another scaling function $\tilde{P}$),

$$P_L(s) = L^{\beta/\nu} \tilde{P}(L/\xi, sL^{\beta/\nu}), \qquad L \to \infty,\ \xi \to \infty,\ L/\xi \text{ finite}. \tag{28}$$

Now it is easy to derive the finite-size scaling relations for the moments of the distribution,

$$\langle |s| \rangle_L = L^{-\beta/\nu} \tilde{M}(L/\xi), \tag{29a}$$

$$\chi(L, T) = L^d(\langle s^2 \rangle_L - \langle |s| \rangle_L^2)/k_B T_c = L^{\gamma/\nu} \tilde{\chi}(L/\xi), \tag{29b}$$

$$U_L = 1 - \frac{\tilde{\chi}_4(L/\xi)}{3\tilde{\chi}^2(L/\xi)}. \tag{29c}$$

One immediately finds that the order parameter at criticality behaves as $\langle |s| \rangle_L \propto L^{-\beta/\nu}$, consistent with our previous result Eq. (17). While in the infinite system the susceptibility would diverge as $\chi(\infty, T) \propto |1 - T/T_c|^{-\gamma}$, in the finite system this divergence is rounded off to a finite value, $\chi(L, T_c) \propto L^{\gamma/\nu}$. This "finite-size rounding" of critical anomalies is again a consequence of the fact that phase transitions, strictly speaking, can occur in the thermodynamic limit only.

Equations (28), (29) are a justification for several methods to study critical properties on the basis of Monte Carlo results for finite systems:

(1) "Data collapsing" [61–64, 70, 75, 76]: Studying, for instance, the susceptibility $\chi(L, T)$ for $T > T_c$ and various L, we have a family of curves. Dividing χ by a factor $L^{\gamma/\nu}$ and the reduced temperature $|1 - T/T_c|$ by a factor $L^{-1/\nu}$, the family of curves should "collapse" on a single curve, the scaling function. The disadvantage of this method is that one tries to fit three parameters simultaneously namely T_c, γ, and ν. In addition, one often has to include Monte Carlo "data" for which neither L nor ξ are very large: hence systematic corrections to the asymptotic finite-size scaling expressions, Eqs. (28), (29), occur. These corrections may prevent complete superposition of the curves; moreover the best "fit" may be obtained for estimates γ, ν, T_c being systematically off their true values. Hence the actual accuracy of the method is somewhat hard to ascertain. Nevertheless it has yielded a variety of useful results (e.g., [75, 76]). As an example we present recent work [70] on the susceptibility of the 2-dimensional Ising model at criticality studied as function of the magnetic field, Fig. 3A: in the infinite system, there should be a divergence $\chi \propto H^{-\gamma/(\beta+\gamma)}$ and again in the finite system this divergence is rounded off. Replotting in Fig. 3B $\chi_L/L^{\gamma/\nu}$ versus the scaled field $HL^{(\gamma+\beta)/\nu}$, all curves indeed nicely collapse onto a single function, within the statistical error of these Monte Carlo data. Since for the 2-dimensional Ising model the critical point (T_c, $H = 0$) as well as the exponents ($\gamma = \frac{7}{4}$, $\beta = \frac{1}{8}$, $\nu = 1$) are exactly known [56], there are no adjustable parameters whatsoever. Thus the success of this scaling description of the finite-size rounding of the susceptibility peak is quite remarkable.

(2) "Cumulant method" [66, 73, 77, 79] (sometimes also referred to as "Monte Carlo coarse graining".) In this method one estimates the slope of the function U_{bL} (U_L) at the intersection point U^*, using Eq. (29c) to derive

$$\frac{1}{\nu} = \left. \frac{\ln(\partial U_{bL}/\partial U_L)}{\ln b} \right|_{U^*}. \tag{30}$$

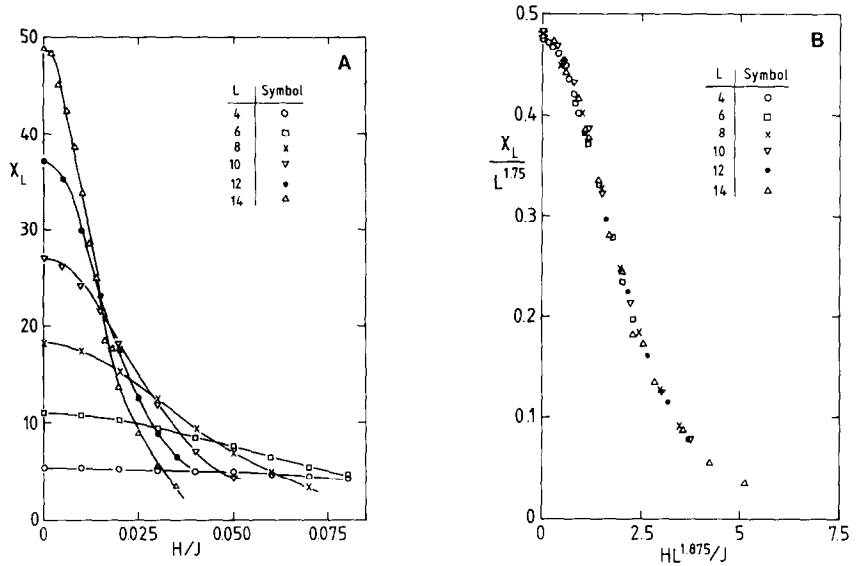

FIG. 3. (A) Susceptibility of 2-dimensional nearest-neighbor Ising square lattices at $k_B T_c/J(\approx 2.269)$ plotted vs magnetic field for various L. (B) Same data as in Fig. 3A replotted as scaled susceptibility vs scaled field. From [70].

Equation (29b) then yields

$$\gamma/\nu = \ln[\chi(bL/T_c)/\chi(L, T_c)]/\ln b. \tag{31}$$

One advantage of this method is that T_c and the exponents are estimated in an independent way; in addition one can analyze systematic errors due to corrections to scaling. Such corrections at T_c to leading order are additive terms with less strongly divergent exponents,

$$\chi(L, T_c) = L^{\gamma/\nu}\tilde{\chi}(0)[1 + \chi^{\text{corr}} L^{-x_{\text{corr}}} + \cdots], \tag{32}$$

χ^{corr} being another amplitude factor and x_{xorr} the leading correction exponent. Unfortunately, careful work on the Ising special purpose processor [16] has revealed that for the 3-dimensional Ising model the asymptotic regime where Eq. (32) is valid is only reached for linear dimensions L exceeding 24 lattice spacings! If one works in this asymptotic regime, then Eq. (31) is replaced by

$$\ln \frac{\chi(bL, T_c)}{\chi(L, T_c)} \Big/ \ln b = \frac{\gamma}{\nu} - \frac{\chi^{\text{corr}} L^{-x_{\text{corr}}}}{\ln b}(1 - b^{-x_{\text{corr}}}). \tag{33}$$

Thus plotting estimates for γ/ν {or $2\beta/\nu$, respectively, cf. [66, 73]} vs $1/\ln b$, one obtains for each L a different curve, which for $(\ln b)^{-1} \to 0$ must extrapolate linearly to the same value of γ/ν. Unfortunately, extremely good statistical accuracy

is required to carry this procedure out. Landau and Binder [75] show that exponent estimates are obtained with an accuracy comparable to the Monte Carlo renormalization group method [38], but the latter technique seems to require less statistical effort. This is also the conclusion of recent Monte Carlo renormalization group work on the 3-dimensional Ising model [82b].

(3) "Phenomenological renormalization" [83]. This technique is also based on Eq. (29b), one studies the temperature dependence of the functions $\varphi_{L,L'}(T)$ and $\varphi_{L',L''}(T)$,

$$\varphi_{L,L'}(T) \equiv \ln[\chi(L', T)/\chi(L, T)]/\ln(L'/L). \tag{34}$$

At T_c the function $\varphi_{L,L'}(T)$ should yield γ/ν (cf., Eq. (31)). Hence the functions $\varphi_{L,L'}(T)$ and $\varphi_{L',L''}(T)$ should intersect at $T_{c'}$; from this intersection point one can read off both an estimate for T_c and an estimate for γ/ν. This method has been applied successfully [83] to the 2-dimensional ANNNI-model, where a transition to an incommensurate floating phase occurs (this transition also is expected to be of the Kosterlitz–Thouless type [80]). In this case it is the wavevector-dependent susceptibility $\chi(L, q, T)$ for which Eq. (34) has to be applied, and one has to vary q to find also the critical wavevector of the incommensurate modulation. This method also requires a rather large statistical effort, since one needs very accurate results for three different lattice sizes to obtain just one estimate for T_c and γ/ν, and in principle one should repeat this analysis for several L to perform the extrapolation towards $L \to \infty$.

The finite-size scaling theory described so far, where one scales the linear dimension L with the correlation length ξ, has the assumption of the hyperscaling relation between the critical exponents $d\nu = \gamma + 2\beta$ built into it [66, 72]. Consequently, finite size scaling in this standard form does not hold when hyperscaling is violated, which happens, for instance, in systems above their marginal dimensionality where mean-field predictions for critical exponents become valid, e.g., for Ising models with $d > 4$ [74]. Since the possibility has been raised that hyperscaling might be violated even for the 3-dimensional Ising model [71] (and for systems in the same universality class, such as gas–fluid critical points, critical unmixing points in binary mixtures, etc.), it is interesting to study size dependencies in the light of such a possible violation of finite-size scaling [16, 71]. In order to achieve this goal, it is crucial, however, to establish what form of scaling replaces finite-size scaling in this more general situation. In [72] it was shown that for systems with periodic boundary conditions one still has a simple scaling form for the free energy of the finite system,

$$f_L = L^{-d}\tilde{F}(tL^{d/(\gamma+2\beta)}, HL^{d(\gamma+\beta)/(\gamma+2\beta)}), \qquad t = (T - T_c)/T_c. \tag{35}$$

This form is of the same type as in the standard case, where Eq. (29) can be found by taking derivatives with respect to the field of the following free energy

$$f_L = L^{-d}\tilde{F}(tL^{1/\nu}, HL^{(\gamma+\beta)/\nu}), \tag{36}$$

and invoking the hyperscaling relation $\{\langle s\rangle_L = -\partial f_L/\partial H,\ \chi(L,T) = -\partial^2 f_L/\partial H^2\}$. In fact, if the hyperscaling relation is true, Eq. (35) simply reduces to Eq. (36). If it is not true, Eq. (35) tells us that the finite size rounding does not set in when L is of order ξ, but rather *L has to be compared with another length, the "thermal" length* $l \propto |t|^{-(\gamma+2\beta)/d}$.

A simple justification of this result (for a more detailed analysis see [72]) can once more be obtained from the probability distribution Eq. (19), noting that for large L, $M_L = Bt^\beta$, $\chi_{(L)} = Ct^{-\gamma}$ where B, C are amplitude factors, and hence the arguments of the exponential functions become

$$\frac{(s \pm M_L)^2 L^d}{2k_B T \chi_{(L)}} = \frac{(st^{-\beta} \pm B)^2 t^{\beta+\gamma} L^d}{2k_B TC} = \frac{(st^{-\beta} \pm B)^2}{2k_B TC} (tL^{d/(\gamma+\beta)})^{\gamma+\beta}. \tag{37}$$

This result shows that indeed t scales with $L^{d/(\gamma+\beta)}$ as anticipated in Eq. (35). Assuming the temperature dependence enters via this thermal length only, Eq. (26) is replaced by

$$P_L(s) = t^{-\beta} P'(L/l, st^{-\beta}) = L^{d\beta/(\gamma+2\beta)} \tilde{P}'(L/l, sL^{d\beta/(\gamma+2\beta)}), \tag{38}$$

which is equivalent to Eq. (35).

These considerations have been checked by Monte Carlo calculations for the 5-dimensional nearest-neighbor Ising model [72], where renormalization group theory predicts the mean-field exponents to be valid [84], $\beta = \frac{1}{2}$, $\gamma = 1$, $\nu = \frac{1}{2}$, and $k_B T_c/J \approx 8.77$ [85]. Thus hyperscaling is strongly violated for $d = 5$. But Fig. 4A shows that the renormalized coupling g_L at criticality indeed tends to constant "fixed point value," in contrast to the suggestion [16] that $g_L \propto L^{-\omega}$, ω being the "anomalous dimension" exponent.

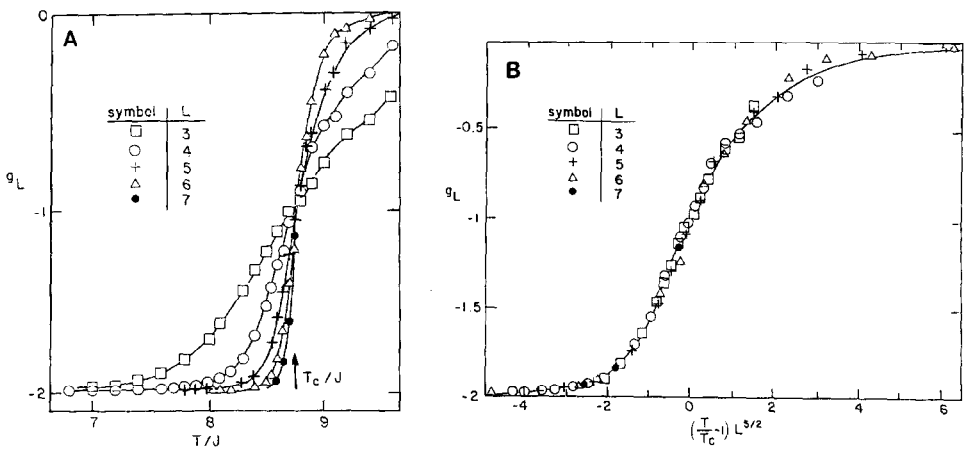

FIG. 4. (A) Monte Carlo results for the renormalized coupling constant g_L of the nearest-neighbor 5-dimensional Ising lattices for various lattice sizes. Arrow shows the high-temperature series expansion for T_c [85]. (B) Same data replotted vs scaled temperature $tL^{5/2}$. From [72].

Figure 4B shows again evidence for scaling by "data collapsing," using $tL^{5/2}$ (Eq. (35)) rather than tL^2 (Eq. (36)) as the scaling variable. This example points towards another advantage of Monte Carlo calculations in general: one can work in arbitrary dimensionalities, which is crucial to test some theories, and of course never possible in laboratory experiments.

Finally we turn to the finite-size effects at first-order phase transitions. In an infinite system a first-order transition is characterized by a delta-function singularity: e.g., if the transition is driven by temperature this singularity is the latent heat; in an Ising magnet, a first-order transition occurs for $T < T_c$ at $H = 0$ driven by the field, and then we get a delta-function singularity in the susceptibility. In finite systems, of course, these delta-function singularities are again rounded off (Fig. 5A) [70]. One can understand this behavior most simply by generalizing Eq. (19) to include the dependence on magnetic field [70],

$$P_L(s) = L^{d/2}(2\pi k_B T \chi_{(L)})^{-1/2} \left\{ \frac{\exp(HM_L L^d/k_B T)}{\exp(HM_L L^d/k_B T) + \exp(-HM_L L^d/k_B T)} \times \exp\left[- \frac{(s - M_L - \chi_{(L)} H)^2 L^d}{2k_B T \chi_{(L)}} \right] + \frac{\exp(-HM_L L^d/k_B T)}{\exp(HM_L L^d/k_B T) + \exp(-HM_L L^d/k_B T)} \times \exp\left[- \frac{(s + M_L - \chi_{(L)} H)^2 L^d}{2k_B T \chi_{(L)}} \right] \right\}. \tag{39}$$

This expression yields the magnetization as follows,

$$\langle s \rangle_L = \chi_{(L)} H + M_L \tanh\left(\frac{HM_L L^d}{k_B T} \right), \tag{40}$$

and the susceptibility becomes (see also [69])

$$\chi(H, T, L) = \frac{\partial \langle s \rangle_L}{\partial H} = \chi_{(L)} + M_L^2 \frac{L^d}{k_B T} \Big/ \cosh^2(HM_L L^d/k_B T). \tag{41}$$

Equation (41) shows that the delta-function singularity, which occurs for $H = 0$ in the limit $L \to \infty$, for finite L is smeared out into a peak of height proportional to L^d and of width ΔH proportional to L^{-d}. Similarly, at a first-order transition driven by temperature the latent heat singularity of the specific heat will be smeared out, and one should observe a peak of height proportional to the volume L^d, with a width ΔT in temperature proportional to the inverse of the volume.

It is important to realize, however, that these considerations apply only if one records the true equilibrium behavior of the system. For too short observation time one would observe a single-peak structure rather than the correct double-peak

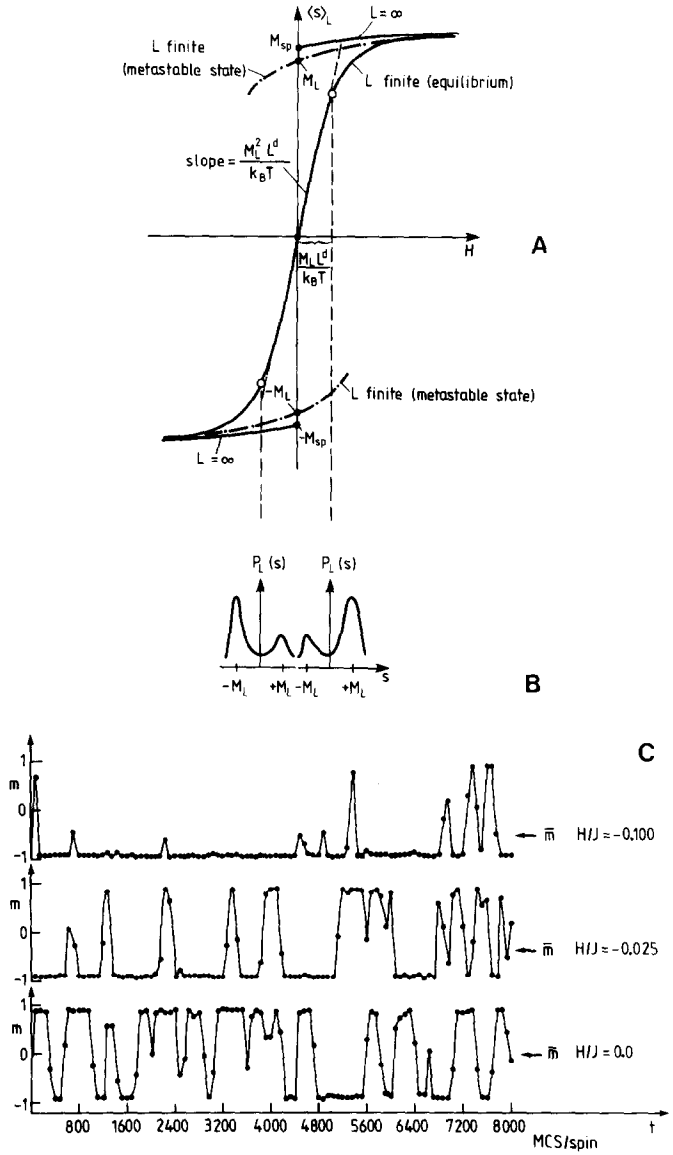

FIG. 5. (A) Schematic variation of magnetization $\langle s \rangle_L$ in a finite Ising ferromagnet plotted vs magnetic field, as observed in thermal equilibrium (full curve) and in a Monte Carlo simulation with short enough observation time where metastable branches occur (dash-dotted curve). The behavior of the infinite system also is indicated. The spontaneous magnetization of the infinite system in denoted by $\pm M_{sp}$, while the most probable value of the magnetization in the finite system at $H=0$ is $\pm M_L$. (B) Schematic probability distribution $P_L(s)$ of the magnetization s for two cases where the magnetization has values in between $\pm M_L$ (open circles in Fig. 5A). (C) Time evolution of the magnetization $m(t)$ plotted vs observation time t (measured in Monte Carlo steps [MCS] per spin) in an Ising nearest-neighbor square lattice of linear dimension $L=6$ with periodic boundary conditions at a temperature $k_B T/J = 2.1$ below T_c, for three values of the field H. Estimates for $\langle s \rangle_L$ as obtained from time averages $\bar{m}$ of $m(t)$

structure and the ordered state is even metastable in a weak field of opposite direction in our example of the field-induced transition in an Ising magnet (Fig. 5). In fact, for using Eqs. (39)–(41) to analyze the Monte Carlo results the sampling time must be so large that many transitions back and forth between the two states have occurred (Fig. 5C), in order that one can estimate reliably the relative weight of the two peaks. In practice this happens only if either the transition is only weakly of first order, or one studies rather small systems. But the advantage of this first-principle method for the study of first-order phase transitions is that it yields unambiguous information on both the location of the first-order transition (from the position of the peak which becomes a delta-function as $L \to \infty$) and the magnitude of the jump (or area underneath the delta-function, respectively). In the present example of the Ising magnet with pairwise interactions this is no real problem, since by symmetry the transition must occur for $H = 0$. But already if a 3-spin interaction would be included, the transition no longer occurs for $H = 0$; similarly, the location of the transition is a problem already for Ising antiferromagnets in a field, etc. With rather short observation times one usually observes rather broad hysteresis loops. It is clear that there does not exist any "equal-area rule" and that the true transition cuts the loop into halfs of equal area: the actual extent of metastability of the two states observed in the simulation is mainly determined from kinetic considerations (of the associated master equation of the model, Sects. 6, 7), rather than by equilibrium thermodynamics. In fact, one does expect a pronounced asymmetry of the hysteresis if one of the two states is ordered but the other one disordered: usually the disordered state is metastable over a broader regime, because it takes a longer time to create a mono-domain ordered state out of an initially disordered one, rather than to destroy the ordered state by thermal fluctuations.

Finally, Fig. 6 shows that the present method based on Eqs. (39)–(41) actually works for the Ising model, at least at not too low temperatures. Although the rounding of the susceptibility peak (Fig. 6A) looks qualitatively similar to that observed at a second-order transition (Fig. 3A), the scaling plot of these data (Fig. 6B) agrees nicely with the explicit scaling function in Eq. (41), and clearly the size-dependence comes in only with trivial factors L^d and there are no other non-trivial exponents, as would occur in the finite size scaling at a second-order transition (Fig. 3B).

We can summarize these results about the finite-size rounding at phase transitions as follows: at a second-order transition, the rounding sets in when the correlation length ξ (if hyperscaling is valid) or the thermal length l (Eq. (35)) (if hyperscaling is not valid), become comparable with the linear dimension of the system. At a first-order transition, there is no diverging length, of course. There finite-size rounding becomes important on a scale of the typical relative mean-square fluctuation of the considered intensive variable (temperature, or—in our case—magnetic field) in a finite volume. This mean-square fluctuation is inversely proportional to the volume. We also remark that finite size scaling is a useful tool for the Monte Carlo study of dynamic critical phenomena, too.

There are also other kinds of finite-size effects which may be important even

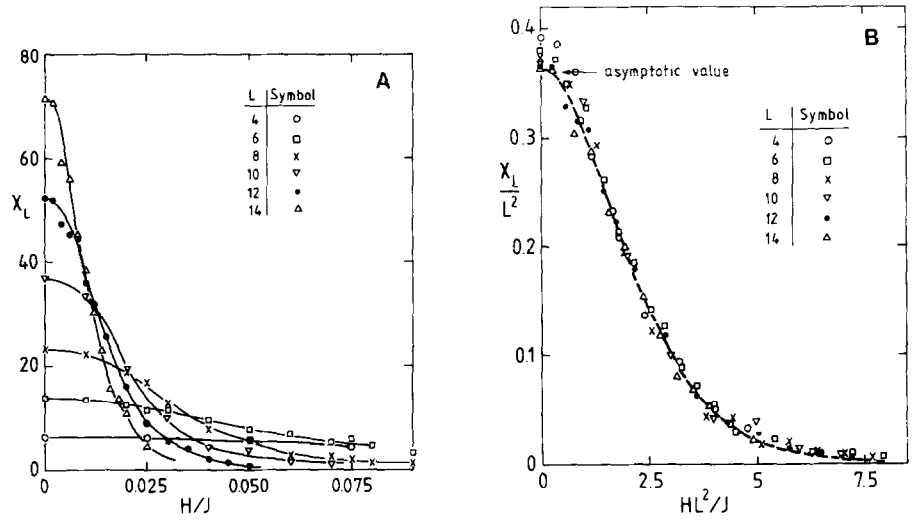

FIG. 6. (A) Susceptibility $\chi(H, T, L)$ of Ising nearest-neighbor square lattices at $k_B T/J = 2.1$ plotted vs magnetic field for various L. (B) Same data replotted in scaled form, $\chi(H, T, L)$ plotted vs scaled field HL^2/J. Arrow indicates the asymptotic value $M_{sp}^2 J/k_B T$ calculated from the exact solution [56]. Dash-dotted curve is the scaling function of Eq. (41), where $\chi_{(L)}$ is omitted. From [70].

under conditions far away from phase transitions. One obvious point applies to cases where the system exhibits long-range order: then the linear dimension L must be commensurate with the long-range order; otherwise the ordered state would be distorted, for instance by creation of interfaces. Of course, this condition creates trouble if one deals with long period superstructures or even orderings which are incommensurate with the lattice. Such incommensurate orderings do occur even in simple Ising-type models, such as the axial-next-nearest-neighbor-Ising (ANNNI-) model, where along one lattice direction a ferromagnetic nearest-neighbor interaction competes with an antiferromagnetic next-nearest-neighbor interaction [86]. In such a case, it is necessary to perform a series of calculations with a series of neighboring large linear dimensions in the lattice direction where this incommensurate modulation occurs.

Another consequence of the finite size together with the periodic boundary condition is the discreteness of **k**-space: the only points in **k**-space where wave-vector dependent correlation functions can be studied are given by

$$\mathbf{k}_\nu = \frac{2\pi}{L}(\nu_1, \nu_2, \ldots, \nu_d), \qquad \nu_1, \ldots, \nu_d = \pm 1, \pm 2, \ldots, \pm L, \tag{42}$$

where we again assumed a cubic system with all linear dimensions equal to L, of course. This discreteness of **k**-space is particularly cumbersome in studies of kinetic quantities, when one wishes to estimate transport coefficients (Sect. 6) or studies the kinetics of ordering (how Bragg peaks develop, Sect. 7) or unmixing processes [87]. Even for equilibrium properties, this discreteness of k-space matters when

there are important long-wavelength excitations which significantly would contribute to some thermodynamic properties of the system. For instance, in an Heisenberg ferromagnet below T_c the spin-waves which have energies proportional to k^2 for small $\mathbf{k}$ are known to give rise to a divergent susceptibility for $H=0$ [88]. Since the largest wavelength a spin-wave can have in a finite system is L, this divergence also is rounded off [89].

Another case where finite-size effects are very important occurs when the system for $N \to \infty$ would correspond to a state within a 2-phase coexistence region. This happens in the study of fluids at constant density ρ, when either the temperature is below critical and ρ lies in between the densities of the gas branch and the liquid branch of the gas–liquid coexistence curve, or for densities in between the fluid density at crystallization and the solid density at melting. It also happens in studies of binary alloys AB at constant relative concentration C_B, which undergo unmixing transitions, if C_B lies in between the concentration values at the coexistence curves $C_{\text{coex}}^{(1)}$, $C_{\text{coex}}^{(2)}$. In the thermodynamic limit, the equilibrium state then consists of a macroscopic mixture of phases. Their relative amounts is given by the lever rule: e.g., for the mixture, the relative amount of phase 2 is given by $[C_B - C_{\text{coex}}^{(1)}]/[C_{\text{coex}}^{(2)} - C_{\text{coex}}^{(1)}]$ and $[C_{\text{coex}}^{(2)} - C_B]/[C_{\text{coex}}^{(2)} - C_{\text{coex}}^{(1)}]$ for phase 1. In a finite system, this is not exactly true, since a nonnegligible fraction of the system then belongs to the interfacial region between the two phases—if the linear dimension is large enough to allow phase separation within the system at all. In addition, there will be a correction of relative order L^{-1} to the energy, for instance, because of the energy cost associated with the interface, and related corrections are obtained for other quantities, too. While a Monte Carlo study of 2-phase coexistence can be of intrinsic physical interest, see Sect. 4, in general it is preferable to avoid this situation: the main reason why this inhomogenous situation is unfavorable is not the existence of the interfacial corrections, but the equilibration problem: if one brings the system from a 1-phase region to a 2-phase region, it usually takes a very large time until the phase separation reaches its final equilibrium state, where just one domain of the minority phase coexists with a surrounding background of the majority phase. Before that state is reached, the system is slowly evolving in time through states containing many "droplets" of the minority phase which gradually coarsen. While such a study of phase separation kinetics is again of interest to elucidate dynamic mechanisms such as nucleation and growth, spinodal decomposition, domain coarsening, etc. [90], for a study of equilibrium properties this slow equilibration clearly is very unfavorable. In addition, the final equilibrium state is strongly fluctuating both with respect to the size and the shape of the minority domain [91], and accurate results then need very large statistical samples.

This problem of 2-phase coexistence is avoided if one uses a statistical ensemble which has intensive variables only (rather than extensive ones such as ρ and C_B one must use the conjugate variables, chemical potential, or chemical potential difference between the two species A, B, respectively). In the thermodynamic limit, the results obtained in these grandcanonical ensembles anyway are equivalent to those obtained from the corresponding canonical ensemble. For finite systems, we never

need worry about interfacial corrections in the grandcanonical ensemble: the 2-phase coexistence region there only shows up as a "forbidden region," in which one never observes stable equilibrium states. Even metastable states (which would lie inside the coexistence curve) are still homogeneous: if sufficiently large minority phase domains were already nucleated in them, they would quickly lead to a decay of the metastable state. Of course, when one studies a first-order transition by sampling suitable probability distributions, as mentioned above, the transitions from one peak of the probability distribution to the other one just correspond to passages of the system through the "forbidden" 2-phase region (Fig. 5).

4. Monte Carlo Study of Systems Containing Surfaces or Interfaces

One interesting application of Monte Carlo calculations is the study of intrinsically inhomogeneous systems. Standard problems are the study of small particles with free surfaces [92, 93] or thin films [61]. Usually one idealizes this situation just by the use of free boundary conditions (in all lattice directions in the case of small particles, in one lattice direction only for thin films). It is, of course, possible to study arbitrary prescribed external shapes of the small particle [92]. Also, one may use any desired inhomogeneities in the interactions, e.g., Ising ferromagnets with exchange interactions J_s differing in the surface layer from their value J in the bulk [94, 96]; one might study surfaces on which local fields act, or where the interactions are disturbed by randomly placed impurities, etc.

In some of these studies, one may be mainly interested in local properties of the first surface layer (of the first few layers) only. This is particularly true if the surface undergoes a phase transition at a temperature different from the transition in the bulk. Then an obvious method for improving the efficiency of the program is an "inhomogeneous sampling" [95–97]: rather than sampling uniformly all lattice sites which are considered for a trial move, one may choose some probability distribution which is peaked in the surface region and sample the lattice from that distribution. In typical cases, lattice sites at the surface may be visited 10 times more often than sites in the bulk. As a typical example of such an application, Fig. 7 shows the temperature dependence of the magnetization m_1 in the surface layer of an Ising ferromagnet for a variety of values of J_s/J.

The Monte Carlo study of interfaces between coexisting phases is less straightforward. Again we concentrate on simple Ising systems to point out the basic problems involved. One problem is to "localize" the interface in the system. The standard first-principle method to do this is to work with a system with free boundaries, where on one half of the boundary sites one applies a suitable magnetic field pointing up, on the other half the field is pointing down: or, equivalently, we may assume that the spins neighboring the boundary are partly fixed at $+1$, partly at -1. Therefore this is referred to as the "fixed spin-boundary condition," Fig. 8a. This boundary condition does indeed create an interface between the two domains

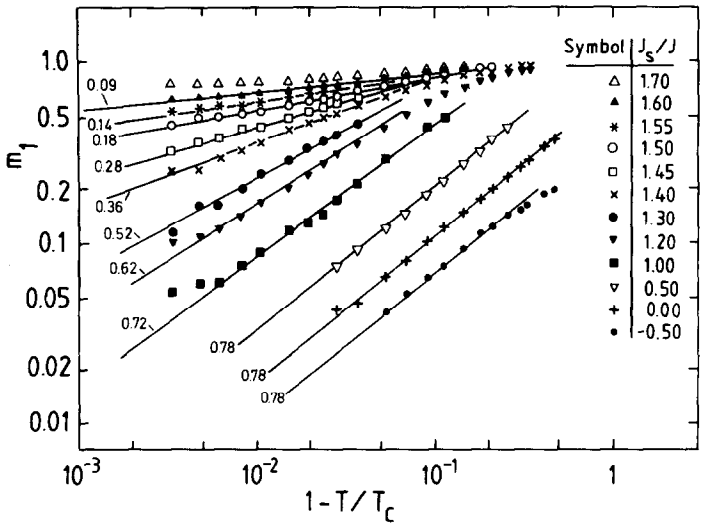

FIG. 7. Log–log plot of surface layer magnetization vs reduced temperature, for various ratios of the exchange J_s in the surface plane to the exchange J in the bulk. Slopes of the straight lines, as indicated, yield effective exponents β_1^{eff}. Most data are based on simulations of a simple cubic Ising lattice of size $50 \times 50 \times 40$, with two free 50×50 surfaces and otherwise periodic boundary conditions. From [95].

of opposite magnetization in the system. However, while the interface clearly is localized at the boundary of the system where the fixed spins of opposite orientations meet, it is not localized in the interior: the contour separating the region of "spin up" from the region of "spin down" makes typical excursions of order $\pm W_d(L)$ in the center of the system, with

$$W_d(L) \propto L^{1/2} \ (d=2) \qquad \text{and} \qquad W_d(L) \propto (\ln L)^{1/2} \qquad (d=3,\ T > T_R). \quad (43)$$

For $d=3$ in Ising systems this behavior only occurs for temperatures exceeding the roughening temperature T_R [98]. Thus the thickness $W_d(L)$ of the interfacial region depends on the thickness L of the system, and diverges in the thermodynamic limit. This phenomenon is the well-known instability of the interface due to long wavelength excitations ("capillary waves") [99].

Now the fixed-spin boundary condition clearly is inconvenient for Monte Carlo calculations: the fixed boundary spins will affect the local magnetization over a distance ξ from the boundary, and hence the domains can only attain their bulk magnetization in the center of $L \gg \xi$; only then we expect the interface to have properties similar to those occuring in the thermodynamic limit.

So what is usually done is to apply the fixed spin boundary condition at two opposite boundaries only; the interface then forms in between and on the average is parallel to these boundaries (Fig. 8b). Then still it is necessary that the linear dimension M perpendicular to the interface is very large; but L now no longer

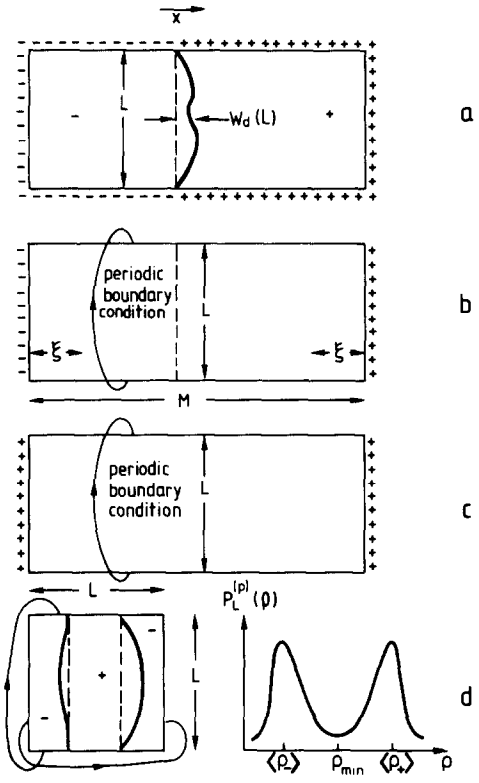

FIG. 8. (A) Boundary conditions for a 2-dimensional Ising system which lead to the formation of an interface below the critical point: spins are fixed at ± 1 as indicated at the boundaries. Thick solid line denotes the (coarse-grained) position of the interface between the phases with negative and positive magnetization in a typical spin configuration. (B) Standard boundary conditions for the computer simulation of a system containing an interface. Note that the linear dimensions $M \gg 2\xi$, where ξ is the bulk correlation length of order-parameter fluctuations. (C) Boundary for a reference system without an interface. (D) Finite system with all boundary conditions periodic and its order-parameter distribution function $P_L^{(p)}(\rho)$. The minimum of $P_L^{(p)}(\rho)$ corresponds to a situation with two interfaces, while the maxima correspond to pure phases with order parameters $\langle \rho_- \rangle$ and $\langle \rho_+ \rangle$, respectively. From [42].

needs to be so large, and one applies periodic boundary conditions in the direction (s) parallel to the interface. A disadvantage of this method is, however, that now the interface thickness not only depends on L but also on M: in fact, keeping L finite one asymptotically expects that $W_d(L) \propto M$ as $M \to \infty$: the interface must not come too close to the fixed-spin boundaries (it must stay away from those a distance at least of order ξ), but otherwise there is no mechanism which would fix it anywhere in the system. Although this geometry has been used for the study of interfacial profiles [100], we feel that this application lacks justification.

But this geometry clearly is useful if we just want to sample interfacial excess quantities, such as the interfacial excess energy, or—in "multistate" models—the

interfacial net adsorbed "mass" of a different state [101]. One then performs a second calculation with fixed-spin boundary conditions at the two opposite planes having the *same sign*, but otherwise identical conditions. In this way one prepares a "reference system" which does not contain an interface (Fig. 8c). Subtracting then the energy obtained with this geometry from the energy obtained with the geometry of Fig. 8b, one obtains the interfacial excess energy. This technique has been used successfully for the 3-dimensional Ising model [100, 102]. As an example, Fig. 9A gives the temperature variation of the interface free energy, which was obtained [102] from the interface internal energy by thermodynamic integration methods (see Sect. 5). It is seen that one can estimate by this technique the interface energy and free energy for the full temperature range, from very low temperatures up to the critical region. The method does become inaccurate very close to the critical point, however: it is well known that the interface free energy F_s must vanish at the critical point [99], while according to [102], F_s there is still positive (albeit small).

An alternative method for obtaining F_s in the critical region was suggested in [42]. This method again is based on the probability distribution of the order parameter, noting that for $s \approx 0$, Eq. (19) no longer holds, but rather the system is dominated by configurations containing two interfaces (Fig. 8d). Thus Eq. (19) in this regime must be replaced by

$$P_L(s \approx 0) \propto P_L(s \approx M_L) \exp(-2L^{d-1} F_s / k_B T), \qquad L \gg \xi, \tag{44}$$

and hence one can estimate F_s directly from sampling $P_L(s \approx 0)$ and attempting suitable extrapolations, such as

$$\frac{F_s}{k_B T} = \lim_{L \to \infty} [\ln P_L(s \approx 0)/2L^{d-1}] = \lim_{L \to \infty} [\ln\{P_L(s \approx 0)/P_L(s \approx M_L)\}/2L^{d-1}]. \tag{45}$$

This approach has been tested for the 2-dimensional nearest-neighbor Ising model [42] and favorable agreement with the exact results for F_s [56] was obtained. Figure 9B shows then the corresponding results for the 3-dimensional simple-cubic nearest-neighbor Ising model [42]. Clearly, F_s obtained by this method does vanish at T_c, as it should, and moreover allows estimation of its critical behavior: the observed critical exponent of 1.32 ± 0.07 is consistent with the value expected from the scaling relation ($2\nu \approx 1.26$ [103a]); moreover the associated critical amplitude $\hat{F}_s \approx 1.05 \pm 0.05$ has been estimated for the first time [42]. This amplitude factor enters several universal amplitude ratios, and the resulting estimates for those are in reasonable agreement with estimates obtained from experiments on fluids such as SF_6, Xe, and CO_2 in the critical region (for a more detailed discussion, see [42]). Very recently, by a rather different multistage sampling method [103b] a presumably even more reliable estimate $\hat{F}_s \approx 1.19 \pm 0.04$ was obtained, improving the agreement with experiment. Thus, although the Ising models emphasized in this review are an oversimplification of any real material, they do have certain "universal" aspects which may directly be compared to experiment.

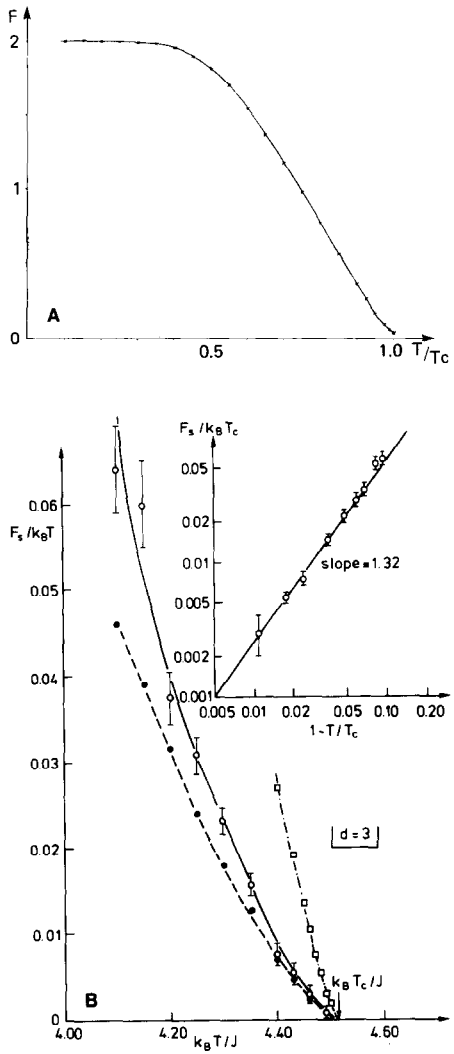

FIG. 9. (A) Interfacial excess free energy of the 3-dimensional simple cubic nearest-neighbor Ising ferromagnet plotted vs temperature. From [102]. (B) Surface tension of the simple-cubic nearest-neighbor Ising model plotted vs temperature in the critical region. Full circles result from the slope of $\ln P_L(0)$ vs L^2, using blocks with periodic boundary conditions, while squares result from the slope of $\ln P_L(0)$ vs L^2 for subsystem blocks. Open circles are the more reliable data resulting from the extrapolation according to Eq. (44). The insert shows a log-log plot of F_s/k_BT_c vs $1 - T/T_c$, to indicate

A related application is the simulation of fluid droplets coexisting with surrounding supersaturated gas. This is a problem of great interest for nucleation theory [104]. Much effort has been spent in simulating droplets of fluids with realistic interactions [104, 105, 93]. Most of these approaches are only valid at rather low temperatures. For the much simpler lattice gas model, it has been possible to devise methods which are valid at all temperatures, up to the critical point [41]. We only discuss this latter problem here, because it also provides a nice application of a technique due to Meirovitch and Alexandrovicz [106] for sampling the chemical potential μ in a simulation at constant density ρ.

If a droplet of finite radius R coexists with surrounding gas, the chemical potential is enhanced in comparison with its value μ_{coex} at the gas–fluid coexistence curve. Observation of this well-known surface effect (Fig. 10) allows one to infer the surface-free energy of the droplets as a function of their radius (Fig. 11) (for details of this analysis, see [41]). Unfortunately, the droplet is strongly fluctuating both in size and shape [41, 91] and hence it is hard to obtain meaningful accuracy. Thus the data shown in Fig. 11 may be preliminary.

Alternative methods for studying the free energy of droplets are based on fluctuation theory, assuming that the concentration of droplets of size l is related to their formation free energy F_l via $n_l = \exp(-F_l/k_B T)$. Given some definition from which droplets can be identified in any microscopic configurations of the system, one has to sample n_l for the range of values of l of interest. This approach, first attempted in [107], has the merit that it easily can be extended to dynamic problems: e.g., one can follow the time-dependence of the droplet number population $n_l(t)$ during a phase change [93, 108], etc. Of course, all these approaches have to fight two difficulties: (i) the first difficulty is the ambiguity in the microscopic definition of droplets, even for the lattice gas model [109]. (ii) The second difficulty is that for cases of experimental interest $F_l/k_B T$ would be very large and then n_l is extremely small, and thus it is very difficult to sample n_l reliably. The first studies of this problem [107] were restricted to $n_l \geqslant 10^{-7}$, with multispin cording techniques and very efficient droplet counting programs it now is possible to go three orders of magnitude further, $n_l \geqslant 10^{-10}$ [110]. Still, it is the opinion of the present author that even further efforts are necessary, in order to finally clarify how F_l varies with droplet size. It is felt, that approaches like "droplet counting" and simulation of gas-droplet coexistence are rather complementary to each other, and combining them might present a more complete picture.

A question of fundamental importance for the theory of first-order phase transition kinetics [111] is the significance of the so-called "spinodal curve." This curve can be defined as the locus of inflection points of the function $F_L(\rho)$ in the temperature-density plane, $F_L(\rho)$ being the coarse-grained free energy of a subsystem of linear dimension L, in which the density is constrained at the value ρ. With the techniques discussed in this article, the inflection point of $F_L(\rho)$ could be obtained in two ways: using the thermodynamic relation $\mu \equiv (\partial F_L/\partial \rho)_T$, and neglecting the distinction between the free energy of a subsystem and that of a single finite system with periodic boundary conditions, the inflection point of F_L is just the maximum

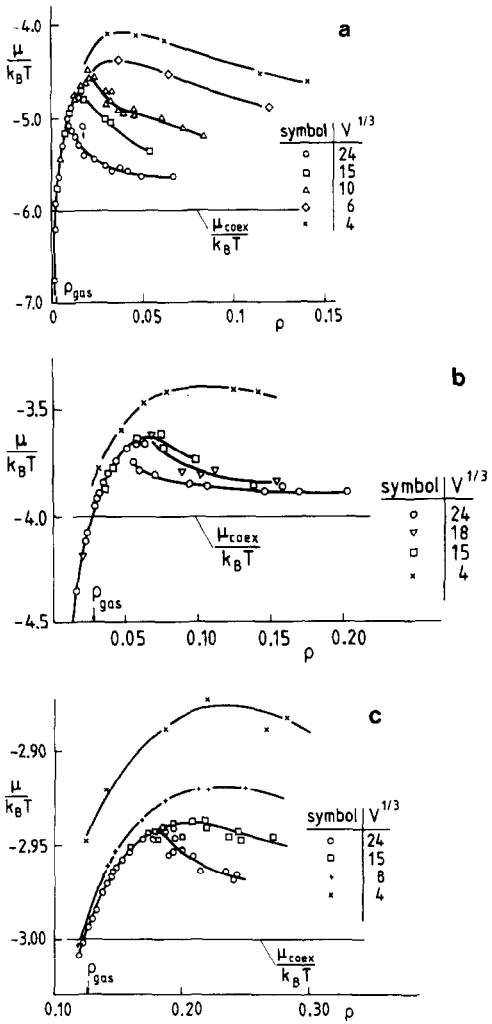

FIG. 10. Chemical potential μ plotted vs density ρ in the simple-cubic nearest-neighbor lattice gas model for $k_BT/J = 2.0$ (a), 3.0 (b), and 4.0 (c). Monte Carlo data for various values of the total volume V are shown (lengths being measured in units of the lattice spacing). Curves are only drawn to guide the eye. The horizontal lines indicate the (exactly known) chemical potential for bulk 2-phase coexistence. From [41].

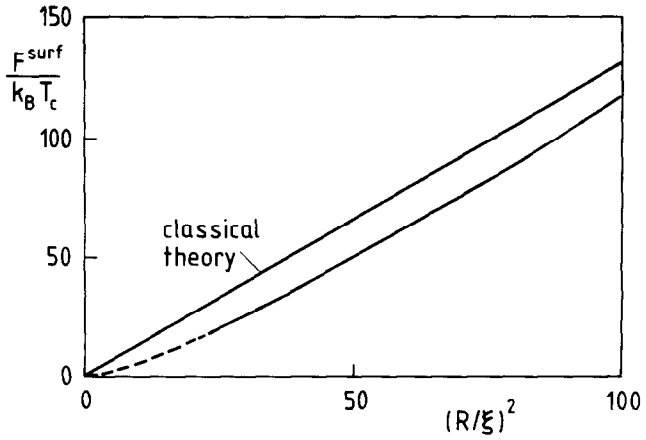

FIG. 11. Surface free energy of droplets in the critical region of the lattice gas model plotted vs the squared droplet radius (measured in units of the bulk correlation length ξ), as calculated in [41] from data such as shown in Fig. 10. The straight line is the result of the classical "capillarity approximation" (i.e., surface tension being independent of droplet radius and hence identical to that of an infinite flat planar interface). From [41].

of μ observed in Fig. 10 for various choices of L and T. Alternatively, we may identify the probability distribution of the density in finite subsystems, which corresponds to the order parameter probability distribution discussed in Sect. 3, as $P_L(\rho) \equiv \exp(-L^d F_L(\rho)/k_B T)$, and hence obtain estimates for the inflection point of $F_L(\rho)$ from sampling $P_L(\rho)$. Figure 12 shows that combining these two approaches one can obtain the location of the inflection point ρ_s for a wide range of L/ξ. In the region where both methods overlap the agreement is satisfactory. Note that by combining a range of different temperatures in this scaling plot it is possible to span a parameter range L/ξ from $L/\xi \approx 0.2$ to $L/\xi \approx 50$, which would never be possible at a single temperature.

We emphasize this example about the spinodal curve here, because it illustrates several ingredients of a successful implementation of the Monte Carlo approach to answer a specific question, in this case the question "how does the inflection point ρ_s of the free energy $F_L(\rho)$ of a subsystem depend on L?": First of all, one must realize that a relevant intrinsic length scale also for this problem is the correlation length ξ of density fluctuations at the gas–fluid coexistence curve. Second, one may use different approaches for the regime $L/\xi \gg 1$ and the regime $L/\xi \approx 1$: for $L/\xi \gg 1$, interactions between different subsystems across their boundaries anyway should be negligibly small, and thus it suffices to consider a single system with $L/\xi \gg 1$. Since $P_L(\rho \approx \rho_s)$ is negligibly small in comparison with $P_L(\rho \approx \rho_{max})$ in this region, we have to constrain the system treating ρ as the independent variable. An important ingredient is then the knowledge of how to sample the conjugate intensive thermodynamic variable, the chemical potential μ [106]. A further useful idea is that for the problem of finding ρ_s one does not need to know $F_L(\rho)$ explicitly, but

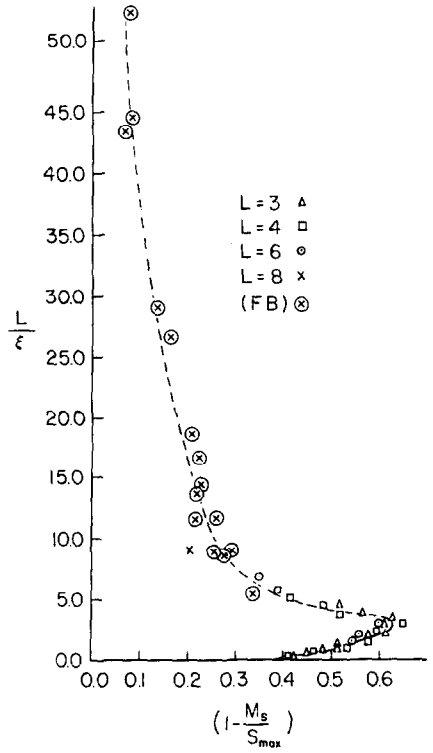

FIG. 12. Scaling plot of the "magnetization" $M_s = 1 - 2\rho_s$ at the spinodal curve (normalized by the "magnetization" $S_{max} = 1 - 2\rho_{max}$, where $P_L(\rho)$ is maximal) vs the linear dimension L measured in units of the correlation lengths. Points labelled with various values of L were taken from $P_L(\rho)$, while points marked *FB* were taken from [41] (maxima of μ in Fig. 10). From [79].

location of the maximum of μ as a function of ρ is sufficient. Conversely, in the regime $L/\xi \approx 1$ the sampling of $P_L(\rho)$ is more practical.

As a final remark of this section, we describe the idea behind sampling the chemical potential for lattice gas models [106]. For simplicity, we only assume nearest-neighbor interaction. Now one introduces the concept of a "local state." This is the state a single lattice site can take, depending on the environment with which exists a direct interaction. Each lattice site can either be empty or occupied by an atom, and an energy $-\varphi$ is won if two neighboring sites are occupied. Hence on the simple cubic lattice the interaction energy can take the seven values $E_\alpha = 0$, $-\varphi, \ldots, -6\varphi$, which define the local states α of an atom at a site. We define a set of seven conjugate states α' by removing the central atom of each state α, with $E_{\alpha'} = 0$. If the frequencies of occurrence of the local states α and α' are denoted as γ_α and $\gamma_{\alpha'}$, the condition of detailed balance requires that [106]

$$\gamma_\alpha/\gamma_{\alpha'} = \exp[(-E_\alpha + \mu)/k_B T)], \qquad \frac{\mu}{k_B T} = \ln(\gamma_\alpha/\gamma_{\alpha'}) + E_\alpha/k_B T. \tag{46}$$

To smooth out fluctuations it is advisable to average μ over all (seven) local states with appropriate weights. Similar ideas can be used in microcanonical calculations, where one wishes to calculate the temperature of the system [39].

Of course, the concept of "local states" is less useful for systems with continuous degrees of freedom, such as for a gas–fluid system. In this case the chemical poten-

$U_{t,N}$, then

$$(\mu - \mu_0)/k_B T = -\ln\langle \exp(-U_{t,N}/k_B T)\rangle_{T,N,V}, \tag{47}$$

μ_0 being the chemical potential of an ideal gas at the same temperature T. Monte Carlo work on this and related problems can be found in [113–120].

5. Simulation of Free Energy and Entropy

As we have seen in Section 2, the importance sampling Monte Carlo method yields information on quantities which are thermal averages of observables, but it does not yield any estimates for the partition function Z itself. As a result, while the internal energy $U = \langle \mathcal{H} \rangle$ is easily calculated, neither free energy $F = -k_B T \ln Z$ nor entropy $S = (U - F)/T$ are obtained directly. Of course, knowledge of F is important particularly when stable states need to be distinguished from metastable ones, by checking which one has lower free energy; this is a problem which frequently occurs for systems undergoing first-order phase transitions from one state to another, and due to hysteresis problems it is then not so easy to even locate the transition with modest accuracy. Thus, this problem has found a lot of attention recently; in the following we briefly survey some of the approaches which have been suggested, and try to discuss their merits.

(i) The method of Salsburg *et al.* [121]: Consider for simplicity, again an Ising Hamiltonian $\mathcal{H}_I$. Then the "volume of phase space" Ω for the partition function $Z = \mathrm{Tr} \exp(-\mathcal{H}_I/k_B T)$ simply is the number of states 2^N the spins $\{S_1, \ldots, S_N\}$ can take, and hence

$$\langle \exp(\mathcal{H}_I/k_B T)\rangle = \frac{1}{Z} \sum_{\text{all states}} 1 = \frac{\Omega}{Z} = \frac{2^N}{Z}. \tag{48}$$

If it is possible to sample $\exp(\mathcal{H}_I/k_B T)$, $\langle \exp(\mathcal{H}_I/k_B T)\rangle \approx (1/M) \sum_{\nu=1}^{M} \exp[\mathcal{H}(\mathbf{X}_\nu)/k_B T]$, constructing a Markov chain of points $\{\mathbf{X}_\nu\}$ as usual, Eq. (48) would yield an estimate for Z. Unfortunately, this method can work for rather small N only: since $\exp(\mathcal{H}_I/k_B T)$ is not extensive but varies exponentially fast with N, $\mathcal{H}_I$ being extensive, the integrand just fluctuates too strongly over too many orders of magnitude.

(ii) Thermodynamic integration method (see, e.g., [122, 57, 123–125]): Here one explores the fact that derivatives of the free energy are easily sampled, and free-energy differences between states can be obtained by integrating over intermediate states. For instance, for an Ising magnet relations which can be explored are

$$U = -T^2[\partial(F/T)/\partial T]_H, \qquad M = -(\partial F/\partial H)_T, \qquad (\partial S/\partial T)_H = (\partial U/\partial T)_H/T, \quad (49)$$

and hence

$$S(T, H) = S(T_1, H) + \int_{T_1}^{T} (\partial U/\partial T)_H \, dT/T, \tag{50a}$$

$$\frac{F}{k_B T} = \frac{U}{k_B T} - \frac{S(T_1, H)}{k_B} - \int_{T_1}^{T} (\partial U/\partial T)_H \, dT/k_B T, \tag{50b}$$

$$\frac{F}{k_B T} = -\frac{S(T_2, H)}{k_B} + \int_{1/k_B T_2}^{1/k_B T} U d(1/k_B T), \tag{50c}$$

$$S(T, H) = S(T_2, H) + U/T - k_B \int_{1/k_B T_2}^{1/k_B T} U d(1/k_B T), \tag{50d}$$

$$F(T, H) = F(T, H_1) - \int_{H_1}^{H} M \, dH. \tag{50e}$$

Thus one needs to know the entropy at the reference state ($\{T_1, H\}$, $\{T_2, H\}$, or $\{T, H_1\}$, respectively) and to calculate U (or M, respectively) at all states in between the reference state and the considered state at (T, H), along the considered path. Of course, the choice of the path is arbitrary and in practice dictated by computational convenience (see, e.g., [124] for a discussion of this point with practical examples). Often the entropy is known only for rather trivial reference states (e.g., $T_1 = 0$, $1/T_2 = 0$, $H_1 \to \infty$). Although the method even then is practically useful (see Fig. 13 for a typical example), often a higher accuracy would seem desirable. Sometimes the accuracy can be improved by using a reference state closer to the regime of interest, where exact low temperature series or high temperature series are available and describe the internal energy still accurately [125]: then one does not need to invest much Monte Carlo effort in an uninteresting region of the phase diagram, and the method is more economical.

(iii) Ma's method [126] of coincidence counting of states along the trajectory in phase space: This method is conceptually much more interesting than the methods mentioned so far. It also can be applied [127] for nonequilibrium problems, such as models of spin glasses where there is a history-dependence and the above integration method involves serious questions [128]. The basic idea is related to the statistical definition of the entropy in terms of the probability p_ν that state $\mathbf{X}_\nu$ occurs,

$$S/k_B = -\sum_\nu p_\nu \ln p_\nu. \tag{51}$$

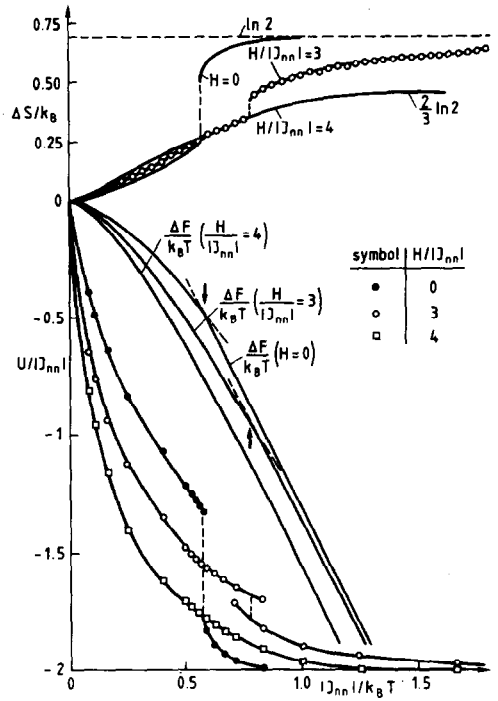

FIG. 13. Internal energy and free energy {lower part} and entropy difference $\Delta S = S(\infty, H) - S(T, H)$ {upper part} of the face-centered cubic Ising antiferromagnet with nearest-neighbor exchange J_{nn} plotted vs inverse temperature. Three values of the magnetic field are shown. Note that for the case where hysteretic first-order transitions occur the location of the transition was adjusted such that $\Delta S(0) = k_B \ln 2$. For $H/|J_{nn}| = 4$ no transition was found and the ground state is a point of finite entropy, which from this work is roughly estimated as $(k_B \ln 2)/3$. From [124].

In principle, p_ν could be estimated from the trajectory as the fraction of time spent in the state $\mathbf{X}_\nu$. In practice, this would work only if the number of states is small enough so that the time spent in each state is long enough to define p_ν accurately. Thus one modifies the approach as follows: One separates the states into groups labeled by λ. Let τ be the total time of the trajectory and τ_λ the time which the trajectory spends in states of the group λ. Then $P_\lambda = \tau_\lambda/\tau$ is the probability of finding a state belonging to group λ. Then

$$S/k_B \approx \sum_\lambda P_\lambda \ln(1/R_\lambda), \tag{52a}$$

where R_λ is the probability of finding a state along the trajectory to coincide with a given state in the group λ. If there are Γ_λ states in the λ phase space, and one assumes that the states in each group are uniformly distributed, then

$$R_\lambda = P_\lambda/\Gamma_\lambda, \tag{52b}$$

Γ_λ being estimated as $\Gamma_\lambda = N_{t\lambda}/N_{c\lambda}$, $N_{t\lambda}$ being the number of trials in each group, and N_{ct} is the coincidence count.

The separation into groups depends on the particular problem. For instance, λ may label the energy intervals. The crucial point, however, is the assumption of uniform probability of the states: this is only true for states far apart along the trajectory (or at least farther apart than the "relaxation time" of the system). Only coincidences of states more distant than this relaxation time must be included in the coincidence count.

Thus Eq. (52), which is a sort of coarse-grained version of Eq. (51), is not so straightforward to apply (at least it is not straightforward to judge the accuracy). A test of Eq. (52) for the 1-dimensional Ising model, however, looks rather encouraging.

(iv) The "stochastic models"-method of Alexandrowicz [129]. This method is not based on standard importance sampling, but rather it is a variant of Monte Carlo methods where one attempts to construct just one "typical" configuration of the system, based on adding particles to previously empty volume, according to certain probabilities which contain several parameters. These parameters are optimally chosen by minimizing the resulting free energy functional; this procedure at the same time yields an estimate for the free energy. Results obtained so far look rather encouraging, and the method seems even to work well right at the critical point of Ising systems [129], where the conventional sampling is plagued by slow relaxation problems. However, unlike the standard procedure, this method does *not* yield answers which are, in principle, exact, and its systematic error—although it seems very small in the cases studied so far—seems hard to ascertain in the general case. Probably this is the reason why this method is not yet widely used, although it certainly is potentially very interesting. At this point, we do not give a detailed description of the method, but refer the reader to the original literature [129].

(v) The "local states"-method due to Meirovitch [130, 131]. This method can also be viewed as an approximation to Eq. (51), where instead of taking the probability p_ν of the state $\mathbf{X}_\nu$ describing the configuration of the total system, one considers probabilities of "local states" I: take in an Ising system a spin (which can be either $+$ or $-$) and a certain group of its neighbors. The various states the neighbors can take are the states labeled by I. The probability that a state $(I, +)$ occurs be $P_{I,+}$ and the probability that $(I, -)$ occurs be $P_{I,-}$. Then

$$S/k_B \cong -\sum_I [P_{I,+} \ln\{P_{I,+}/(P_{I,+} + P_{I,-})\} + P_{I,-} \ln\{P_{I,-}/(P_{I,+} + P_{I,-})\}]. \quad (53)$$

Clearly, if the cluster of spins taken for the description of the local state is made bigger and bigger, the approximation should converge towards the exact answer, Eq. (51). In practice this method is limited, of course, by the exponential increase which then results in the number of local states which has to be sampled. But in a certain range the definition of what is a "local state" can in practice be varied [130, 131] and thus, from the scatter of the various estimates obtained, one gets an

idea about the magnitude of the systematic error. The results obtained so far are most encouraging [130, 131]. In particular, the problem of ordering on the face-centered cubic Ising antiferromagnet in a field with nearest-neighbor interaction, which has been mentioned above as an example for the application of the thermodynamic integration method, has been treated recently with the "local states" technique as well [131]. It seems that (with somewhat larger statistical efforts) one can obtain considerably more accurate results: e.g., comparing estimates for S for 8 different choices of the local states Meirovitch concludes that the ground-state entropy for $H = 12\,|J_{nn}|$ is [131] $S/k_B = 0.24989$ (2); if correct, this estimate has two more significant digits than the estimate obtained by thermodynamic integration [124]! For $H = 4\,|J_{nn}|$, Meirovitch obtains [131] $S/k_B \approx 0.239$ (1) rather than [124] $S/k_B \approx (\ln 2)/3 \approx 0.231$: thus in unfavorable cases, where the convergence of the "local states"-method is slow, its accuracy is probably not much

improved, and in nearly all cases studied so far reasonably accurate estimates seem to result from calculations with rather small clusters of neighbors defining a "local state."

(vi) "Multistage sampling" [132] and "umbrella sampling" [133]. These methods are based on a consideration of the energy distribution $p(U)$,

$$p(U)\,dU = (1/Z)\exp[-\mathscr{H}(\mathbf{X})/k_B T]\,d\mathbf{X}. \tag{54}$$

By importance sampling one obtains only the normalized distribution, however,

$$p_n(U) \equiv p(U) \Big/ \int dU\, p(U), \tag{55}$$

and thus the information on the normalization factor $(1/Z)$ in Eq. (54) is lost. However, if the system size is sufficiently small one can study parts of $p(U)$ directly with sufficient accuracy by simple sampling. If one obtains a sufficiently broad region of U, where both $p(U)$ (by simple sampling) and $p_n(U)$ (by importance sampling) can be obtained, a comparison of the two distributions obviously yields the partition function. The disadvantage of this technique can again be seen very clearly for an Ising model: the distribution $p(U)\exp[\mathscr{H}(\mathbf{X})/k_B T]$, with which the points $\mathbf{X}$ are chosen in the simple sampling run, is peaked at $U = 0$ with a width of order $1/\sqrt{N}$; similarly, $p_n(U)$ is peaked at $U_N = \langle \mathscr{H} \rangle$ with a width of order $1/\sqrt{N}$: thus the simple sampling can yield data only far out in the wings of $p_n(U)$, where it is hard to get reasonable statistics. This problem is dealt with [132] by generating intermediate "bridging distributions."

A more elegant way of handling this problem is to recall [2] that one may choose phase space points $\mathbf{X}_\nu$ wth any prescribed, nonphysical, probability $p(\mathbf{X}_\nu)$, rather than according to $p(\mathbf{X}_\nu) \propto \exp\{-\mathscr{H}(\mathbf{X}_\nu)/k_B T\}$ as in the usual importance

sampling method. Then thermal averages are no longer simple arithmetic averages but rather [2]

$$\langle A \rangle \approx \bar{A} = \frac{\sum_{\nu=1}^{M} A(\mathbf{X}_\nu) \exp[-\mathscr{H}(\mathbf{X}_\nu)/k_B T]/P(\mathbf{X}_\nu)}{\sum_{\nu=1}^{M} \exp[-\mathscr{H}(\mathbf{X}_\nu)/k_B T]/P(\mathbf{X}_\nu)}. \tag{56}$$

Choosing $P(\mathbf{X}_\nu)$ in a clever way one can get very good statistics into the wings of the energy distribution $p_n(U)$ [133]. These methods now are standard tool in the context of simulations of fluids [8, 11], where usually one treats systems with rather small particle number, and then the method is practically useful. Unlike the methods previously discussed, "umbrella sampling" gets more difficult the larger the size of the system.

As a general conclusion of this section, we remark that several routes exist by which entropy and free energy can be obtained from Monte Carlo simulation. Some of these techniques (such as the methods of Ma [126] and Meirovitch [130]) are very beautiful from a conceptual point of view, but their application seems to be useful mainly for systems with discrete degrees of freedom. Others (like umbrella sampling [133]) become impractical for very large particle number. Thus, it depends on the problem under consideration which of the methods described above is most efficient.

6. Monte Carlo Studies of the Dynamics of Fluctuations near Equilibrium (Diffusion) Problems, etc.

As mentioned in Section 2, the Monte Carlo method can be viewed as a numerical realization of a dynamic evaluation of a system described by master equation. Hence the Monte Carlo process can be taken as a simulation of corresponding physical situations, for which a description in terms of a master equation is appropriate. An example for this situation is provided by diffusion processes in solids: e.g., in an interstitial alloy, the diffusion of the interstitials may be modelled by a stochastic hopping between the available lattice sites. Since the mean time between two successive jumps is orders of magnitude larger than the time scale of atomic vibrations in the solid, the phonons can be reasonably well approximated as a heatbath, as far as the diffusion is concerned. (Of course, there are also cases where this approximation gets unreliable, such as superionic conductors: for their realistic simulation the techniques described here are not sufficient, and molecular dynamics methods are needed.)

In the last few years there has been large activity in this field, and the various results obtained have recently been extensively reviewed [43, 134]. Therefore, the present section will be rather brief.

As always in a Monte Carlo simulation of a dynamic model, one first has to appropriately specify the transition probability $W(\mathbf{X} \to \mathbf{X}')$ in the master equation for the probability $P(\mathbf{X}, t)$ that state $\mathbf{X}$ occurs at time t,

$$\frac{d}{dt}P(\mathbf{X}, t) = -\sum_{\mathbf{X}'} W(\mathbf{X} \to \mathbf{X}')\, P(\mathbf{X}, t) + \sum_{\mathbf{X}'} W(\mathbf{X}' \to \mathbf{X})\, P(\mathbf{X}', t). \tag{57}$$

For a problem of diffusion in a lattice gas, the transition $\mathbf{X} \to \mathbf{X}'$ typically consists of a jump of a particle to an empty nearest-neighbor lattice site; but it would also be possible to consider jumps to more distant sites, of course, and allow different attempted jump rates for different distances. In addition, one may wish to consider systems containing also different kinds of particles with different rates, or where the jump rates in different directions of the lattice are not equivalent (anisotropic diffusion).

In the simplest case of only one kind of particle present and isotropic diffusion we may write the transition probability for nearest-neighbor jumps as follows, using the notation in terms of occupation variables $\{c_i = 0, 1\}$ for the lattice sites i appropriate for lattice gas models,

$$\tau_s W(c_i \to c_{1_i}) = \frac{c_i}{\langle c \rangle}(1 - c_{1_i})\, f_T^{(i)}. \tag{58}$$

Here the factor $c_i(1 - c_{1_i})$ accounts that only particles ($c_i = 1$) can jump, and the transition probability is zero if the neighboring site 1_i is already occupied. The time constant τ_s is a factor setting the time scale, while $f_T^{(i)}$ is a "thermal" factor ensuring detailed balance with the chosen Hamiltonian. For noninteracting problems, $f_T^{(i)}$ may simply be put equal to unity. Of course, the detailed balance condition does not specify $f_T^{(i)}$ uniquely. A choice taken in the case of nearest-neighbor interaction ε is [134, 135]

$$\begin{aligned} f_T^{(i)} = \exp(-\Delta E/k_B T), \qquad \Delta E &= \varepsilon(k - Z + 1) \qquad (\varepsilon < 0), \\ &= \varepsilon k \qquad\qquad\quad (\varepsilon > 0), \end{aligned} \tag{59}$$

where Z is the coordination number, and k the number of neighbor sites of i which are already occupied. Another choice is [136, 137]

$$f_T^{(i)} = \exp[-\delta\mathscr{H}/2k_B T]/(\exp[\delta\mathscr{H}/2k_B T] + \exp[-\delta\mathscr{H}/2k_B T]), \tag{60}$$

$\delta\mathscr{H}$ being the energy change associated with the jump. Of course, if microscopic information on the jump process and its rates were available, it could be used as an input for the Monte Carlo simulation. In the absence of such knowledge or other physical considerations dictating the choice of $f_T^{(i)}$, this choice is rather arbitrary.

The quantities commonly calculated in the context of "self diffusion" studies are the number of performed jumps $\langle W \rangle$ per unit time and per particle and the mean square displacement $\langle r_i^2(t) \rangle$ of particles as a function of time. Here the angular brackets are understood as time average according to the master equation Eq. (57), e.g.,

$$\langle r_i^2(t) \rangle = (t_M - t - t_0)^{-1} \int_{t_0}^{t_M - t} [\mathbf{r}_i(t + t') - \mathbf{r}_i(t')]^2\, dt'. \tag{61}$$

In addition, statistics are gained by taking an average over all particles i; t_0 is the initial time of the averaging (and of the equilibration run) and t_M the total time over which the run is extended. Equation (61) then yields the self-diffusion constant D_s of the d-dimensional lattice with N sites,

$$D_s = \lim_{t \to \infty} \left[\sum_i \langle r_i^2(t) \rangle / (2dN \langle c \rangle t) \right]. \tag{62}$$

One also introduces a correlation factor f by the following definition (valid for cubic crystals with lattice spacing a)

$$D_s \equiv \langle W \rangle f a^2. \tag{63}$$

Another quantity of interest for incoherent neutron scattering is the dynamic self correlation function

$$S_{\text{inc}}(\mathbf{q}, t) = (1/N\langle c \rangle) \sum_{\text{all particles } i} \langle \exp[i\mathbf{q} \cdot \{\mathbf{r}_i(0) - \mathbf{r}_i(t)\}] \rangle. \tag{64}$$

It is also possible to define and evaluate more sophisticated quantities such as the "waiting time distribution function" [138] but this is outside of our consideration here. We only mention a simple technical point related to the evaluation of distances $\mathbf{r}_i(t+t') - \mathbf{r}_i(t')$ needed in Eq. (61): in a finite system with periodic boundary conditions particles will disappear on one side of the system and reappear on the opposite one. In order to avoid unphysical finite-size effects due to such effects, one may use two sets of coordinates for each particle: the first set is used for the basic finite lattice and is used for selecting particles for a move, computing the transition probability W, etc. The second set agrees with the first one for time $t = 0$, but is not restricted to the basic cell at later stages: thus then a coordinate $\mathbf{r}_i(t)$ at later stages may be an image of the particle in the basic cell generated by the periodic boundary conditions. Thus when a particle moves through the surface of the basic cell to a neighboring cell, we do not change its coordinate of the second set by $\pm L$ (L being the linear dimension of the system), as one does for the first set of coordinates. Thus the distance $|\mathbf{r}_i(t+t') - \mathbf{r}_i(t')|$ may exceed L by far for late times, which means that the particle has travelled to a rather distant "image" of the basic cell. With this definition of coordinates to be used in Eq. (61) the limit expressed in Eq. (62) trivially exists also for a finite system. The same trick is used for related problems, such as simulation of polymer motion [139].

Somewhat less straightforward to determine is the collective diffusion constant D which measures how a small local density excess spreads out. Various methods for estimating D have been proposed and are briefly reviewed in [43]. Here we only mention the "linear response" method of [136, 137], where one first equilibrates the system in the presence of a perturbation $\delta\mathcal{H}(\mathbf{q})$ in the Hamiltonian,

$$\delta\mathcal{H}(\mathbf{q}) = -\delta\mu \sum_j \cos(\mathbf{q} \cdot \mathbf{r}_j)\, c_j. \tag{65}$$

If the amplitude $\delta\mu$ of this periodic chemical potential variation is small enough, it will lead to a wavelike modulation of concentration given by

$$\delta c(\mathbf{q}) = \chi(\mathbf{q})\,\delta\mu \sum_j \cos(\mathbf{q}\cdot\mathbf{r}_j), \tag{66}$$

where $\chi(\mathbf{q})$ is the "wave-vector dependent susceptibility" (which by this method also can be conveniently sampled).

[redacted]

$$\langle \delta c(\mathbf{q}, t)\rangle = \chi(\mathbf{q}, t)\,\delta\mu \sum_j \cos(\mathbf{q}\cdot\mathbf{r}_j), \qquad \chi(\mathbf{q}, t) = \chi(\mathbf{q}) \exp\{-Dq^2(t-t_0\}, \tag{67}$$

from which result one can extract D. The angular bracket in Eq. (67) in this case means a "nonequilibrium-average" over several equivalent runs, needed to smooth out statistical fluctuations in $\delta c(\mathbf{q}, t)$, which are of order $\sqrt{\chi(\mathbf{q})/N}$ and hence the "noise" is comparable to the "signal" $\langle \delta c(\mathbf{q}, t)\rangle$ except for very large N (note that $\delta\mu$ must be small in order to avoid nonlinear response). In spite of these limitations, this method works reasonably well. At the same time it illustrates a general advantage of all kinds of computer simulations: "thought-experiments" are readily carried out [140]. As an example of the type of work which can be performed, Fig. 14 presents calculations of the self-diffusion constant D_s and the collective diffusion constant D as a function of average concentration or "coverage" $\theta = \langle c\rangle$ for a variety of temperatures, assuming a square lattice gas model with repulsive interactions ϕ_{nn} between nearest neighbors and ϕ_{nnn} between next nearest neighbors, for $\phi_{nn} = \phi_{nnn}$ [137]. The various order–disorder transitions of this lattice gas model show up in the dynamic quantities in a rather complicated way. For an analysis of this behavior we refer to the original literature [137].

We conclude this section by a discussion of criticisms recently raised on the interpretation of Monte Carlo simulations in terms of master equations in general [141]. There it is emphasized that the Monte Carlo process should be viewed as a dynamic evolution with a discrete rather than continuous time increment, $\Delta t = 1/N$ (adopting units of one Monte Carlo step per site). As is well known, discrete dynamical problems often give rise to rather complicated behavior {chaotic time evolution, limit cycles, and other behavior studied in the context of "nonlinear dynamics"}, and the approach to the continuum limit is nontrivial.

However, we feel that this criticism misses some important understanding about the dynamic interpretation of Monte Carlo processes. The point is that the time increment for the Monte Carlo microstep is understood to be $\Delta t = 1/N$ only on the average. Of course, when one calculates time averages of time-displaced correlation functions [e.g., Eq. (61)] the fluctuations of the actual system time relative to the "time" labelling the Monte Carlo microsteps are averaged out. The same holds in Eq. (67) when the ensemble average over many equivalent runs is taken. A more

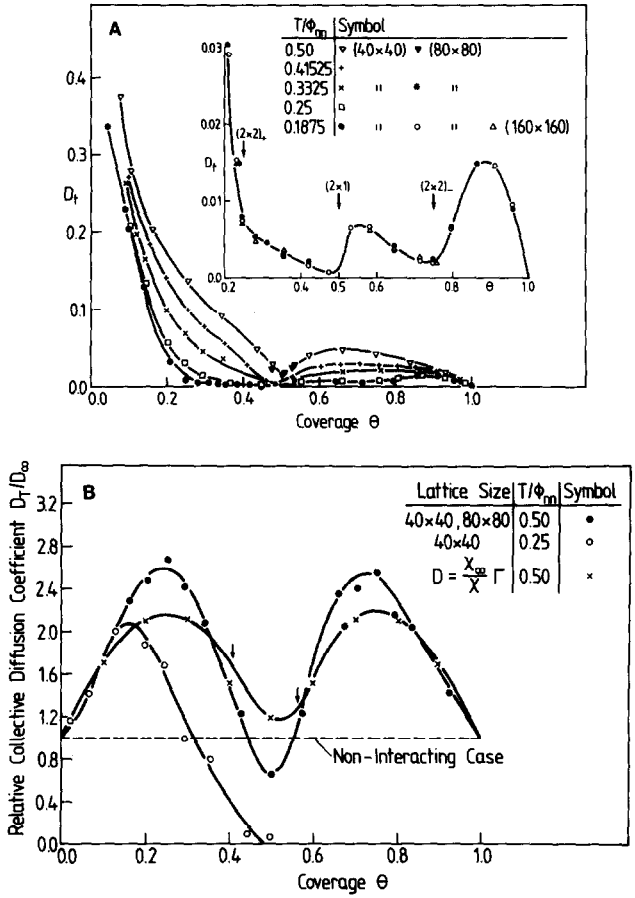

FIG. 14. Self-diffusion constant (A) and collective diffusion constant (B) plotted vs coverage $\theta = \langle c \rangle$ for a variety of temperatures, according to a simulation of square lattice gases with repulsive interactions between nearest and next nearest neighbors, for the case $\phi_{nn} = \phi_{nnn}$. Arrows indicate order–disorder transitions. Various lattice sizes have been used as indicated. From [137].

formal discussion of this problem is given by Serinko [142]. We emphasize also that the actual performance of the Monte Carlo method to sample time-displaced correlation functions of dynamic models has been thoroughly tested for the 1-dimensional kinetic Ising model [50], where the exact solution is known [48]. Very good agreement with the exact results was found [50]. Of course, for the dynamic applications it is essential to select the degrees of freedom for a trial move at random, while for equilibrium properties it is often better to select them in order going regularly through the lattice.

7. Monte Carlo Studies of Processes far from Thermal Equilibrium

A field of Monte Carlo sampling which is particularly expanding is the application to study processes far from equilibrium. Some of those can be viewed as early stages of the approach towards equilibrium: e.g., to this category belong simulations of nucleation phenomena [108], simulations of spinodal decomposition [90, 43] and of the growth of domains of an ordered phase out of a disordered one [43]. As an example, we shall comment on this latter problem below. But we also emphasize that there are other problems which are purely "unidirectional" and have no relation to thermal equilibrium at all: e.g., "kinetic irreversible gelation" (as an example for simulations of this problem, see [143]) or "diffusion-limited aggregation" (e.g., [144]; see [43] for a selected bibliography). There stochastic processes are defined by specifying certain transitions $\mathbf{X} \to \mathbf{X}'$ and transition probabilities $W(\mathbf{X} \to \mathbf{X}')$, but the inverse transition $\mathbf{X}' \to \mathbf{X}$ does not exist and hence there is also no detailed balance principle. For these problems, the lack of analytical approaches makes simulations to be the main source of information, and thus there is an enormous recent activity.

Also with respect to the laws governing the growth of ordered domains, the understanding in terms of analytical theories is quite limited and thus Monte Carlo simulations are very valuable and a lot of recent work hence deals with this problem [145–155]. Again it is not the intention of this review to give an exhaustive discussion of the results obtained so far, and their physical significance; rather we want only to describe how such studies are performed, and what typical problems are encountered. For simplicity, we concentrate on recent work [151, 152] on the square lattice gas with nearest-neighbor repulsion and next-nearest-neighbor repulsion of equal strength, which already has served as an example for diffusion studies in the previous section.

Figure 15 shows "raw data" of such a simulation, where the four different kinds of order in the 2×1 structure are indicated by four different symbols (in this structure, rows of empty sites alternate with full rows: these rows may be oriented parallel to the x axis as well as parallel to the y axis, and they may also be interchanged with one another). It is seen that a variety of domains of rather irregular shapes forms rather quickly after the quench to the considered temperature. These snapshot pictures also illustrate already some of the difficulties of this particular application of Monte Carlo sampling: (i) The domain patterns at different times are highly correlated with each other, thus initial fluctuations in the pattern may get amplified. It is then necessary to average all properties over many equivalent runs, in order to obtain a physically meaningful information. (ii) The domains are very irregular, and sometimes they contain holes which again are filled by domains of other kinds. Hence it is not straightforward to associate a meaningful linear dimension $L(t)$ to these domains. (iii) At later times it may happen that one species of the domains starts to percolate from one boundary of the system through the system right to the other side (the snapshot at $t = 200$ MCS in Fig. 15 is close to such a percolation phenomenon). This percolation phenomenon

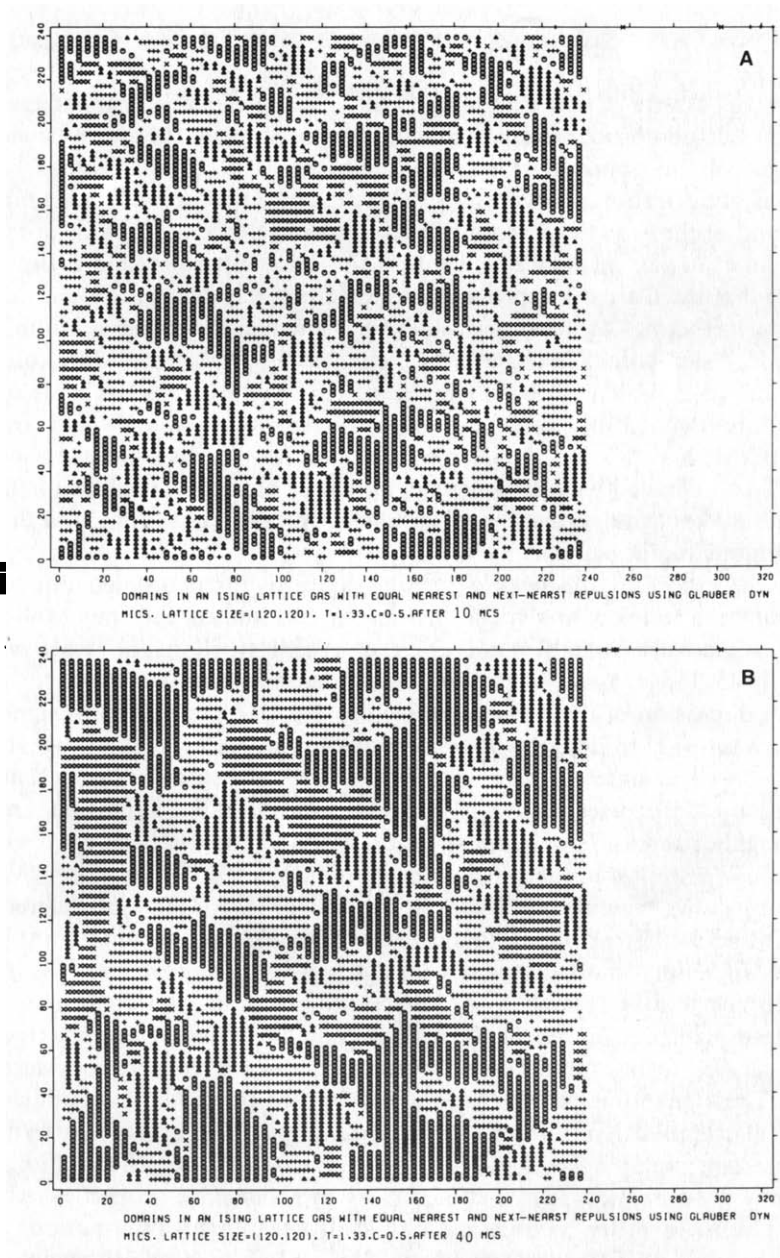

FIG. 15. Snapshot pictures of a 120×120 square lattice gas (with periodic boundary conditions) with nearest- and next-nearest-neighbor repulsive interaction of equal strength, quenched at time $t = 0$ and field $H = 0$ from infinite temperature to $T/|J_{nn}| = 1.33$ (about 64% of the critical temperature). Time evolution follows single-spin flip dynamics. Times shown are at 10 (A), 40 (B), 60 (C), and 200 (D) Monte Carlo steps after the quench. Lattice sites taken by a particle are shown by circles, triangles, standing crosses, or lying crosses, depending on the type of domain to which they belong. From [152].

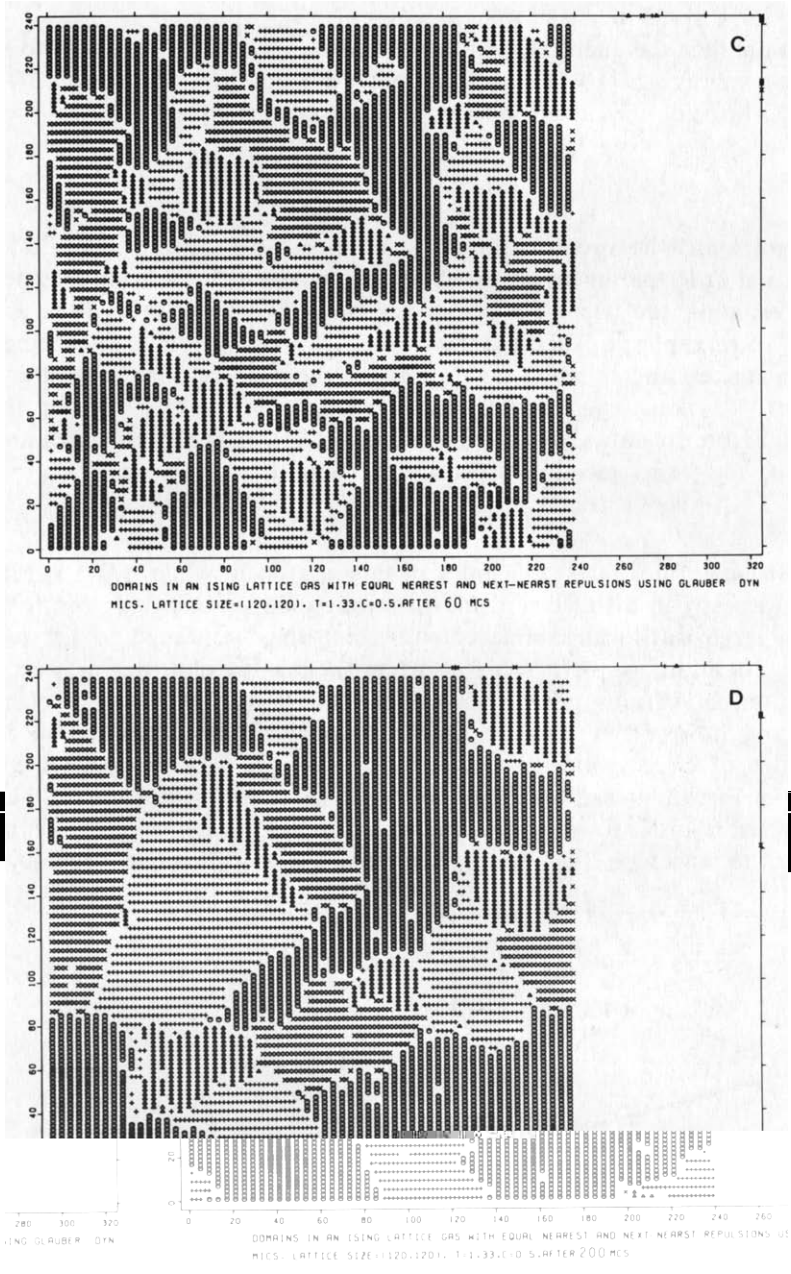

FIGURE 15—*Continued*

is clearly an unwanted finite size effect, which needs to be eliminated by simulating suitably large systems.

What are then the quantities that are "measured"? What is very easy to record, is the excess energy $\Delta E(t) = U(t) - U(\infty)$ and a domain linear dimension $L(t)$ defined by [151] (d being the dimensionality, $d=2$ in our example)

$$[L(t)]^d = \left[\sum_i \psi_i^2(t)\right] N/\langle\psi\rangle_T^2, \tag{68}$$

where $\psi_i(t)$ are the order parameter components at time t, and $\langle\psi\rangle_T$ is the equilibrium order parameter at the temperature to which the quench is performed. In our example, the two order parameter components can be defined as $\psi_1(t) = (1/N)\sum_j S_j(t)\exp[\mathbf{r}_j\cdot\mathbf{q}_1]$ and $\psi_2(t) = (1/N)\sum_j S_j(t)\exp[\mathbf{r}_j\cdot\mathbf{q}_2]$, $S_j(t)$ being the spin variable at site j and at time t, and $\mathbf{q}_1$, $\mathbf{q}_2$ are the reciprocal lattice vectors describing the (2×1) long range order, $\mathbf{q}_1 = \pi(1,0)/a$, $\mathbf{q}_2 = \pi(0,1)/a$, a being the lattice spacing. Figure 16 shows typical results for both $\Delta E(t)$ and $L(t)$, which are presented in log–log form, since one expects power laws [151],

$$L(t) \propto t^x, \qquad \Delta E(t) \propto t^{-y}. \tag{69}$$

Figure 16 again illustrates difficulties of this approach: while $\Delta E(t)$ is rather well behaved already in a single run, $L(t)$ is strongly fluctuating from run to run, and hence a large statistical sample of equivalent runs is needed to get reasonable accuracy. In addition, there is curvature on the log–log plot: this may be due to a competition of various growth mechanisms; it may also be an artefact of the simulation, however: it may be a finite size effect, or attributed to imprecise knowledge of $U(\infty)$ which crucially enters $\Delta E(t)$ at late times. In the example shown in Fig. 16, it has not been possible to properly single out the various possibilities; in order to obtain reasonable data all lattice sizes have been averaged together, to conclude that both exponents $x \approx y \approx 0.36$. The accuracy of this

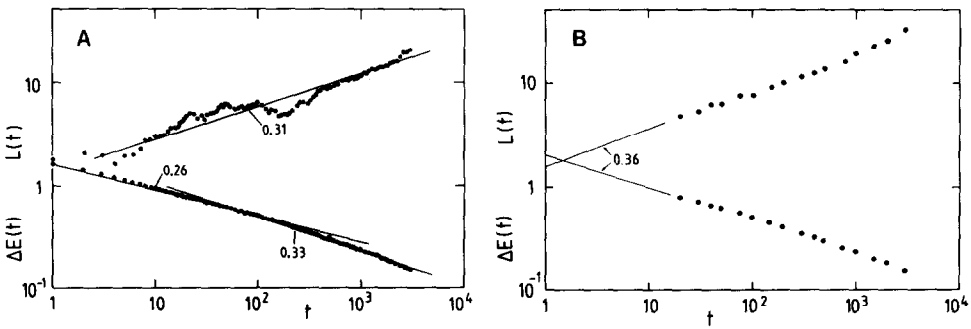

FIG. 16. Log–log plot of $\Delta E(t)$ and $L(t)$ vs time, for the temperature $T/|J_{nn}| = 1.33$ and concentration $\langle c\rangle = \frac{1}{2}$, using a particle hopping dynamics which conserves the concentration (the transition probability Eqs. (57), (59) is used). Case (A) shows an average of 4 runs for 400×400 lattices, while case (B) shows an average over several hundred runs of lattice sizes in the range from 80×80 to 800×800. From [152].

procedure is rather uncertain, however, and analytical arguments were presented [152] in favor of $x = y = \frac{1}{3}$.

Another quantity which is of interest is the structure factor

$$S(\mathbf{q}, t) = \frac{1}{N} \left\langle \left| \sum_j S_j(t) \exp[i\mathbf{q} \cdot \mathbf{r}_j] \right|^2 \right\rangle. \tag{70}$$

Here the angular bracket again indicates that an average over a sample of equivalent runs needs to be performed. The structure factor is hampered by the additional finite size effect, mentioned in Section 2, that $\mathbf{q}$ is restricted to a discrete set of values compatible with the periodic boundary conditions. For q-values in between those, $S(\mathbf{q}, t)$ is unknown, and common practice is to connect $S(\mathbf{q}, t)$ defined at discrete q values in between by straight lines (Fig. 17A). Since $S(\mathbf{q}, t)$ is also plagued by large statistical fluctuations, it is again hard to obtain a meaningful accuracy. Within the rather modest accuracy attainable, one typically finds that $S(\mathbf{q}, t)$ satisfies a scaling property (Fig. 17B) if $S(\mathbf{q}, t)$ is normalized by its maximum value at the Bragg position $\mathbf{q}_{\text{Bragg}}$, and $\mathbf{q} - \mathbf{q}_{\text{Bragg}}$ is normalized by the half width $\delta(t)$ of the peak. Of course, $\delta^{-1}(t)$ can be taken as another quantity measuring the linear dimension of the domains in the system.

In conclusion, although the results of the various studies [145–155] are rather encouraging and clearly provide a first physical insight into the problem, questions of accuracy still need to be studied carefully: one must analyze the finite-size effects as well as the way in which statistical fluctuations depend on sizes of the system and sizes of the statistical sample. The lack of a "self-averaging property" (e.g., $L(t)$ taken from one run of an 800×800 lattice has an order of magnitude larger fluc-

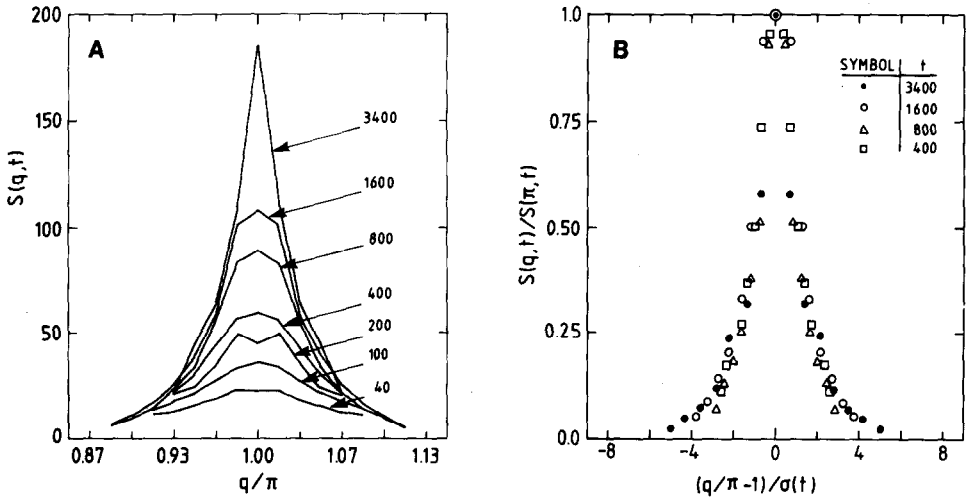

FIG. 17. (A) Structure factor $S(q, t)$ plotted vs q at different times (measured in Monte Carlo steps per particle) for $T/|J_{nn}| = 0.75$, $\langle c \rangle = \frac{1}{2}$, using an average of 235 runs for a 120×120 lattice. (B) Same data replotted in scaled form as indicated in the text. From [152].

tuation than 100 runs of 80×80 lattices, although the total number of sites in both cases is the same [152]) certainly needs theoretical investigation.

8. Conclusions

In this review, it has been shown that one understands rather nicely how to analyze static properties at phase transitions obtained from Monte Carlo simulations: finite-size effects both at second-order and at first-order transitions are well understood, and size-dependence can be used as a tool to both locate a transition and quantitatively estimate corresponding properties. Also the statistical errors with presently available computers can be made reasonably small, such that meaningful studies are possible.

With respect to dynamic properties at phase transitions, the situation is somewhat less encouraging. Although there is much successful work on various aspects of diffusion problems, as mentioned in Section 6, it is still a problem to study critical slowing down at second-order phase transitions: in systems with conserved order parameter, one expects the diffusion constant to vanish; while some qualitative evidence for this phenomenon has been seen by Monte Carlo [136, 156], these studies in quantitative respect still are unsatisfactory. Also the first problem to which dynamic Monte Carlo studies were applied, namely estimating the critical exponent of the relaxation time in the single spin flip kinetic Ising model [4, 50, 157a], is not satisfactorily solved, despite recent efforts [157b]. The recently developed special purpose processores [14, 15] seem to be nicely suited to handle this problem. Recent progress has also been achieved by applying finite size scaling concepts to critical dynamics [157c].

While several applications of dynamic Monte Carlo renormalization group methods to this problem [158a] also did yield somewhat unsatisfactory results, the most recent effort [158b] using a new vectorized multispin coding technique [34] on the CDC Cyber 205 computer ("method of 2^d colours") with a speed of 22×10^6 Monte Carlo updates per second seems to yield, for the first time, estimates for the dynamic exponents with good accuracy.

And a similar situation occurs with respect to dynamic processes far from equilibrium relevant for phase transitions (such as nucleation, spinodal decomposition [90, 43, 108], growth of ordered domains (Sect. 7), etc.): although Monte Carlo simulations have contributed significantly to our understanding of these processes, many important problems are still unsolved, and the precise nature of limitations of simulations due to finite system size and finite size of the statistical sample need to be investigated more closely. It seems likely that with additional efforts along those lines substantial progress in the near future will be possible.

There is one area, however, where the situation must be judged much more pessimistically: this is the field of phase transitions in systems with quenched disorder (models for spin glasses, systems with random fields, etc. [154, 155, 159]). In many cases, it is controversial whether such models have a phase transition at finite

temperature or not. Even such a qualitative question often then cannot be conclusively answered by Monte Carlo simulation either, due to the occurence of very large relaxation times in the system.

As an example of such a problem, we mention the 3-dimensional Ising model with bonds $\pm J$, the signs of which are chosen at random. If a transition to a spin glass phase occurs, one expects the susceptibility $\chi_{EA} = \sum_{ij}[\langle S_i S_j \rangle_T^2]_{av}/N$ to diverge there. (Here the average $[\cdots]_{av}$ means an average over the random bond distribution.) Figure 18 presents typical data for χ_{EA} and the associated correlation length ξ_{EA} [160]. The straight lines shown on these plots illustrate power laws such as $\xi_{EA} \propto T^{-4}$, $\chi_{EA} \propto T^{-12}$, which would imply that there is a phase transition at zero temperature only. However, it is also possible that a phase transition does occur at finite nonzero temperature, in the regime of temperatures somewhat lower than where data points are shown. It is very hard to check this, however: in the regime investigated, the average relaxation time τ increases dramatically upon lowering the temperature, consistent with a law $\ln \tau \propto T^{-4}$. The case where τ is equal to the observation time over which time averages are taken, corresponds to a "dynamic freezing transition" which has nothing to do with a static phase transition in the system. Taking as a time unit $\tau_0 = 1$ MCS/spin, early work found such a transition

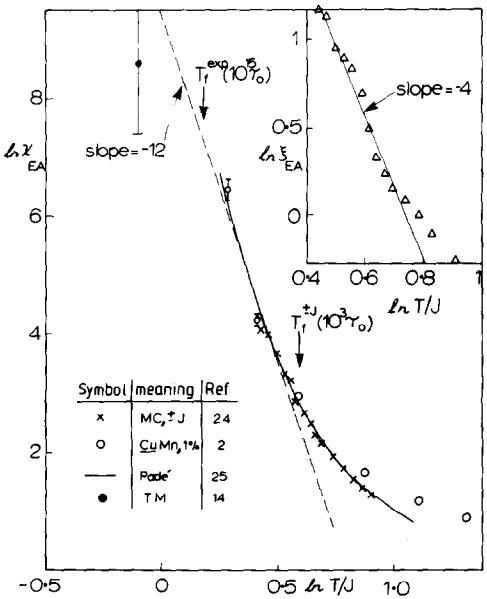

FIG. 18. Log–log plot of χ_{EA} vs T/J for the simple cubic $\pm J$ Ising spin glass. Crosses are Monte Carlo results and the solid curve is a Padé analysis due to R. G. Palmer [private communication] of the series of [163]. The filled circle is a lower bound from a transfer matrix calculation [164]. Arrows mark the freezing temperatures of earlier Monte Carlo work [161] and CuMn 1% experiment [162]. The insert shows ξ_{EA} vs T/J. From [160].

work on Cu Mn 1% spin glasses included in Fig. 18 [162], where $\tau_0 \approx 10^{-12}$ s, the experimental freezing temperature T_f^{exp} would correspond to a time $\tau \approx 10^{15}\tau_0 \approx 10^3$ s. While the Monte Carlo data shown in Fig. 18 span a range of observation times from τ_0 to $10^6\tau_0$, and with special purpose processors one can go up to $10^9\tau_0$ [17], this range is still smaller than the time range accessible in the experiment. Since for glass transitions it seems crucial that a spectrum of relaxation times develops which spans many decades, their study with Monte Carlo methods obviously is rather hard. But even in these cases, the comparison of Monte Carlo simulations with analytical theories and experiment has been rather useful [159].

A detailed analysis of recent data obtained with the Bell Laboratories spin glass special-purpose computer indicates that possibly a transition in this $\pm J$ model does occur at $k_B T_f$ ($J \approx 1.2$) [17]. This conclusion is consistent with another study where the finite size scaling techniques of Sec. 3 are applied to this problem [165]. However, due to the problems mentioned above neither of these studies can settle this issue beyond doubt.

ACKNOWLEDGMENTS

The author is particularly grateful to H. Furukawa, J. D. Gunton, K. Kaski, D. P. Landau, A. Sadiq, and A. P. Young for their fruitful and pleasant collaboration on parts of the work described in this review.

REFERENCES

1. N. METROPOLIS, A. W. ROSENBLUTH, M. N. ROSENBLUTH, A. H. TELLER, AND E. TELLER, *J. Chem. Phys.* **21** (1953), 1087.
2. L. D. FOSDICK, *Methods Comput. Phys.* **1** (1963), 245.
3. K. BINDER AND H. RAUCH, *Z. Phys.* **219** (1969), 201.
4. H. MÜLLER-KRUMBHAAR AND K. BINDER, *J. Stat. Phys.* **8** (1973), 1.
5. For a recent review, see Y. SAITO AND H. MÜLLER-KRUMBHAAR, *in* "Applications of the Monte Carlo Method in Statistical Physics" (K. Binder, Ed.), p. 223, Springer-Verlag, Berlin/Heidelberg/New York, 1984.
6. B. I. HALPERIN AND D. R. NELSON, *Phys. Rev. B* **19** (1979), 2457; *Phys. Rev. Lett.* **42** (178), 121.
7. W. W. WOOD, *in* "Physics of Simple Liquids" (H. N. V. Temperley, J. S. Rowlinson, and G. S. Rushbrooke, Eds.), p. 115, North-Holland, Amsterdam, 1968.
8. J. P. VALLEAU AND S. G. WHITTINGTON, *in* "Modern Theoretical Chemistry, Vol. 5: Statistical Mechanics" (B. J. Berne, Ed.), p. 134, Plenum, New York, 1977; J. P. VALLEAU AND G. M. TORRIE, ibid., p. 169.
9. W. W. WOOD, *in* "Fundamental Problems in Statistical Mechanics," (E. G. D. Cohen, Ed.), Vol. 3, p. 331, North-Holland, Amsterdam, 1975.
10. D. LEVESQUE, J. J. WEIS, AND J. P. HANSEN, *in* "Monte Carlo Methods in Statistical Physics" (K. Binder, Ed.), p. 47, Springer-Verlag, Berlin/Heidelberg/New York, 1979.
11. D. LEVESQUE, J. J. WEIS, AND J. P. HANSEN, *in* "Applications of the Monte Carlo Method in Statistical Physics" (K. Binder, Ed.), p. 38, Springer-Verlag, Berlin/Heidelberg/New York, 1984.
12. H. E. MÜSER, *Ferroelectrics* **39** (1981), 1099.
13. P. BAK, *Phys. Today* (Dec. 1983), 25.

14. R. B. PEARSON, J. L. RICHARDSON, AND D. TOUSSAINT, *J. Comput. Phys.* **51** (1983), 243.
15. A. HOOGHLAND, J. SPAA, B. SELMAN, AND A. COMPAGNER, *J. Comput. Phys.* **51** (1983), 250.
16. M. N. BARBER, R. B. PEARSON, J. L. RICHARDSON, AND D. TOUSSAINT, preprint.
17. A. OGIELSKY, private communication; A. OGIELSKY AND I. MORGENSTERN, preprint.
18. D. C. HANDSCOMB, *Proc. Cambridge Philos. Soc.* **58** (1962), 594; **60** (1964), 115.
19. M. SUZUKI, S. MIYASHITA, A. KURODA, AND C. KAWABATA, *Phys. Lett. A* **60** (1977), 478; M. SUZUKI, S. MIYASHITA, AND A. KURODA, *Prog. Theor. Phys.* **58** (1977), 1377.
20. M. SUZUKI, *Prog. Theor. Phys.* **56** (1976), 1454; *Commun. Math. Phys.* **51** (1976), 183; **57** (1977), 193.
21. J. J. CULLEN AND D. P. LANDAU, *Phys. Rev. B* **27** (1983), 297; A. WIESLER, *Phys. Lett. A* **89** (1982), 359.
22. H. DERAEDT AND A. LAGENDIJK, *Phys. Rev. Lett.* **46** (1981), 77; *J. Stat. Phys.* **27** (1982), 731; *Phys. Rev. Lett.* **49** (1982), 1552; *Phys. Rev. B* **24** (1981), 463.
23. J. W. LYKLEMA, *Phys. Rev. Lett.* **49** (1982), 88; preprint.
24. J. W. LYKLEMA, *Phys. Rev. B* **27** (1983), 3108.
25. D. J. SCALAPINO AND R. L. SUGAR, *Phys. Rev. Lett.* **46** (1981), 519; *Phys. Rev. B* **24** (1981), 4295; J. E. HIRSCH, D. J. SCALAPINO, R. L. SUGAR, AND R. BLANKEBECLER, *Phys. Rev. Lett.* **47** (1981), 1628; J. E. HIRSCH AND M. GRABOWSKI, *Phys. Rev. Lett.* **52** (1984), 1713; J. E. HIRSCH, *Phys. Rev. B* **28** (1983), 4059; *Phys. Rev. Lett.* **51** (1983), 1900; D. SCALAPINO, R. L. SUGAR, AND W. D. TOUSSAINT, *Phys. Rev. B* **29** (1984), 5253.
26. F. FUCITO, E. MARINARI, G. PARISI, AND C. REBBI, *Nucl. Phys. B* **180** (1981), 369.
27. K. BINDER (Ed.), "Monte Carlo Methods in Statistical Physics," Springer-Verlag, Berlin/Heidelberg/New York, 1979.
28. K. BINDER (Ed.), "Applications of the Monte Carlo Method in Statistical Physics," Springer-Verlag, Berlin/Heidelberg/New York, 1984.
29. M. CREUTZ, L. JACOBS, AND C. REBBI, *Phys. Rev. Lett.* **42** (1979), 1390.
30. L. JACOBS AND C. REBBI, *J. Comput. Phys.* **41** (1981), 203.
31. R. ZORN, H. J. HERRMANN, AND C. REBBI, *Comput. Phys. Commun.* **23** (1981), 337.
32. C. KALLE AND V. WINKELMANN, *J. Stat. Phys.* **28** (1982), 639.
33. K. BINDER AND D. STAUFFER, *in* "Applications of the Monte Carlo Method in Statistical Physics," p. 1, Springer-Verlag, Berlin/Heidelberg/New York, 1984.
34. S. WANSLEBEN AND J. G. ZABOLITZKY, preprint; G. O. WILLIAMS AND M. H. KALOS, *J. Stat. Phys.* **37**, 283 (1984).
35. A. B. BORTZ, M. H. KALOS, AND J. L. LEBOWITZ, *J. Comput. Phys.* **17** (1975), 10.
36. K. BINDER (Ed.), "Monte Carlo Methods in Statistical Physics," p. 1, Springer-Verlag, Berlin/Heidelberg/New York, 1979.
37. A. SADIQ, *J. Comput. Phys.* **55** (1984), 387.
38. R. H. SWENDSEN, *in* "Real-Space Renormalization" (T. W. Burkhardt and J. M. J. van Leeuwen, Eds.), Springer-Verlag, Berlin/Heidelberg/New York, 1982; for recent important progress, see R. H. SWENDSEN, *Phys. Rev. Lett.* **52** (1984), 1165; *Phys. Rev.* **B30** (1984), 3866, 3875.
39. M. CREUTZ, *Phys. Rev. Lett.* **50** (1983), 1411; A. SADIQ, *Phys. Rev. B* **9** (1974), 2299.
40. T. L. HILL, "Thermodynamics of Small Systems," Benjamin, New York, 1963.
41. H. FURUKAWA AND K. BINDER, *Phys. Rev. A* **26** (1982), 556.
42. K. BINDER, *Phys. Rev. A* **25** (1982), 1699.
43. K. W. KEHR AND K. BINDER, *in* "Applications of the Monte Carlo Method in Statistical Physics," p. 181, Springer-Verlag, Berlin, 1984.
44. K. BINDER AND D. P. LANDAU, *Surface Sci.* **108** (1981), 503.
45. L. D. LANDAU AND E. M. LIFSHITZ, "Statistical Physics," Pergamon, London, 1979.
46. I. Z. FISHER, *Sov. Phys.-Usp. Engl. Transl.* **2** (1959), 783.
47. K. BINDER, *in* "Phase Transitions and Critical Phenomena" (C. Domb and M. S. Green, Eds.), Vol. 5b, p. 1, Academic Press, New York, 1976.
48. R. J. GLAUBER, *J. Math. Phys.* **4** (1963), 294; for a detailed review, see K. KAWASAKI, *in* "Phase

Transitions and Critical Phenomena" (C. Domb and M. S. Green, Eds.), Vol. 2, p. 443, Academic Press, New York, 1972.
49. M. CREUTZ, *Phys. Rev. D* **21** (1980), 2308.
50. E. STOLL, K. BINDER, AND T. SCHNEIDER, *Phys. Rev. B* **8** (1973), 3266.
51. K. C. BOWLER AND B. J. PENDLETON, *Nucl. Phys. B* **230** (1984), 109.
52. A. P. YOUNG AND S. KIRKPATRICK, *Phys. Rev. B* **15** (1982), 440.
53. D. STAUFFER AND K. BINDER, *Z. Phys. B* **30** (1978), 313; **41** (1981), 237.
54. H. MÜLLER-KRUMBHAAR AND K. BINDER, *Z. Phys.* **254** (1972), 269.
55. H. E. STANLEY, "An Introduction to Phase Transitions and Critical Phenomena," Oxford Univ. Press, Oxford, 1971.
56. B. M. MCCOY AND T. T. WU, "The Two-Dimensional Ising Model," Harvard Univ. Press, Cambridge, Mass., 1973.
57. K. BINDER, *Physica (Amsterdam)* **62** (1972), 508; *Phys. Status Solidi* **46** (1971), 567.
58. M. E. FISHER AND A. E. FERDINAND, *Phys. Rev. Lett.* **19** (1967), 169; A. E. FERDINAND AND M. E. FISHER, *Phys. Rev.* **185** (1969), 832.
59. M. E. FISHER, *in* "Critical Phenomena" (M. S. Green, Ed.), p. 1, Academic Press, New York, 1971; M. E. FISHER AND M. N. BARBER, *Phys. Rev. Lett.* **28** (1972), 1516.
60. K. BINDER AND P. C. HOHENBERG, *Phys. Rev. B* **6** (1972), 3461; **9** (1974), 2194.
61. K. BINDER, *Thin Solid Films* **20** (1974), 367.
62. TH. T. A. PAAUW, A. COMPAGNER, AND D. BEDEAUX, *Physica* **79** (1975), 1.
63. E. DOMANY, K. K. MON, G. V. CHESTER, AND M. E. FISHER, *Phys. Rev. B* **12** (1975), 5025.
64. D. P. LANDAU, *Phys. Rev. B* **13** (1976), 2997; **14** (1976), 255.
65. M. N. BARBER, *in* "Phase Transitions and Critical Phenomena" (C. Domb and J. L. Lebowitz, Eds.), Vol. 8, p. 145, Academic Press, New York, 1983; M. P. NIGHTINGALE, *J. Appl. Phys.* **53** (1982), 7927.
66. K. BINDER, *Z. Phys. B* **43** (1981), 119.
67. Y. IMRY, *Phys. Rev. B* **21** (1980), 2042.
68. M. E. FISHER AND A. N. BERBER, *Phys. Rev. B* **26** (1982), 2507; H. W. J. BLÖTE AND M. P. NIGHTINGALE, *Physica A* **112** (1982), 405; J. L. CARDY AND M. P. NIGHTINGALE, *Phys. Rev. B* **27** (1983), 4256; P. KLEBAN AND C. K. HU, *Bull. Amer. Phys. Soc.* **27** (1982), 92(A); and preprint.
69. V. PRIVMAN AND M. E. FISHER, *J. Stat. Phys.* **33** (1983), 385.
70. K. BINDER AND D. P. LANDAU, *Phys. Rev. B* **30** (1984), 1477.
71. B. A. FREEDMAN AND G. A. BAKER, JR., *J. Phys. A* **15** (1982), L715.
72. K. BINDER, M. NAUENBERG, V. PRIVMAN, AND A. P. YOUNG, *Phys. Rev.* **B31** (1985), 1498.
73. K. BINDER, *Phys. Rev. Lett.* **47** (1981), 693.
74. E. BREZIN, *J. Phys. (Paris)* **43** (1982), 15.
75. K. BINDER AND D. P. LANDAU, *Phys. Rev. B* **21** (1980), 1941; D. P. LANDAU AND K. BINDER, preprint.
76. D. P. LANDAU, *Phys. Rev. B* **27** (1983), 5604.
77. D. P. LANDAU, *J. Magn. Magn. Mat.* **31–34** (1983), 11.
78. C. S. S. MURTY AND D. P. LANDAU, *J. Appl. Phys.* **55** (1984), 2429.
79. K. K. KASKI, K. BINDER, AND J. D. GUNTON, *Phys. Rev. B* **29** (1984), 3996.
80. J. M. KOSTERLITZ AND D. THOULESS, *J. Phys. C* **6** (1973), 1181; J. M. KOSTERLITZ, *J. Phys. C* **7** (1974), 1046.
81. J. V. JOSE, L. P. KADANOFF, S. KIRKPATRICK, AND D. R. NELSON, *Phys. Rev. B* **16** (1977), 1217.
82a. J. TOBOCHNIK, *Phys. Rev. B* **26** (1982), 6201.
82b. G. S. PAWLEY, R. H. SWENDSEN, D. J. WALLACE, AND K. G. WILSON, *Phys. Rev.* **29** (1984), 4030.
83. M. N. BARBER AND W. SELKE, *J. Phys. A* **15** (1982), L617.
84. M. E. FISHER, *Rev. Mod. Phys.* **46** (1974), 587.
85. M. E. FISHER AND D. S. GAUNT, *Phys. Rev. A* **133** (1964), 224.
86. W. SELKE AND M. E. FISHER, *Z. Phys. B* **40** (1980), 71; *J. Magn. Magn. Mat.* **15–18** (1980), 403; W. SELKE, *Z. Phys. B* **43** (1981), 335.

87. J. MARRO, J. L. LEBOWITZ, AND M. H. KALOS, *Phys. Rev. Lett.* **43** (1979), 282; *Acta Metall.* **30** (1982), 297.
88. L. SCHÄFER AND H. HORNER, *Z. Phys. B* **29** (1978), 251 and references therein.
89. H. MÜLLER-KRUMBHAAR, *Z. Phys.* **267** (1974), 261.
90. K. BINDER, M. H. KALOS, J. L. LEBOWITZ, AND J. MARRO, *Adv. Colloid Interface Sci.* **10** (1979), 173.
91. H. FURUKAWA AND K. BINDER, *Phys. Rev. A* **26** (1982), 556; K. BINDER AND M. H. KALOS, *J. Stat. Phys.* **22** (1980), 363.
92. K. BINDER, H. RAUCH, AND V. WILDPANER, *J. Phys. Chem. Solids* **31** (1970), 391; V. WILDPANER, *Z. Phys.* **270** (1974), 215.
93. H. MÜLLER-KRUMBHAAR, *in* "Monte Carlo Methods in Statistical Physics" (K. Binder, Ed.), Chap. 5, presents an overview.
94. K. BINDER AND P. C. HOHENBERG, *Phys. Rev. B* **9** (1974), 2194.
95. K. BINDER AND D. P. LANDAU, *Phys. Rev. Lett.* **52** (1984), 318.
96. K. BINDER AND D. P. LANDAU, to be published.
97. E. EISENRIEGLER, K. KREMER, AND K. BINDER, *J. Chem. Phys.* **77** (1982), 6296.
98. J. D. WEEKS, *in* "Ordering in Strongly Fluctuating Condensed Matter Systems" (T. Riste, Ed.), p. 293, Plenum, New York, 1980.
[redacted]
1983.
100. H. J. LEAMY, G. H. GILMER, K. A. JACKSON, AND P. BENNEMA, *Phys. Rev. Lett.* **30** (1973), 601.
101. W. SELKE, preprint; see also W. SELKE AND W. PESCH, *Z. Phys. B* **47** (1982), 335; W. SELKE AND J. YEOMANS, *J. Phys. A* **16** (1983), 2789.
102. E. BÜRKNER AND D. STAUFFER, *Z. Phys. B* **53** (1983), 241.
103a. J. C. LE GUILLOU AND J. ZINN-JUSTIN, *Phys. Rev. B* **21** (1980), 3976.
103b. K. K. MON AND D. JASNOW, *Phys. Rev. A* **30** (1984), 670; and to be published.
104. For reviews, see "Nucleation" (A. C. Zettlemoyer, Ed.), Dekker, New York, 1969; "Nucleation Phenomena" (A. C. Zettlemoyer, Ed.), Elsevier, New York, 1977; K. BINDER AND D. STAUFFER, *Adv. Phys.* **25** (1976), 343.
105. See, e.g., J. K. LEE, J. A. BARKER, AND F. F. ABRAHAM, *J. Chem. Phys.* **58** (1973), 3166.
106. H. MEIROVITCH AND Z. ALEXANDROVICZ, *Mol. Phys.* **34** (1977), 1027.
107. E. STOLL, K. BINDER, AND T. SCHNEIDER, *Phys. Rev. B* **6** (1972), 2777.
108. K. BINDER AND H. MÜLLER-KRUMBHAAR, *Phys. Rev. B* **9** (1974), 2328; for a review, see K. BINDER AND M. H. KALOS, *in* "Monte Carlo Methods in Statistical Physics" (K. Binder, Ed.), p. 225, Springer-Verlag, Berlin, 1979.
109. K. BINDER, *Ann. Phys. (N.Y.)* **98** (1976), 390; A. CONIGLIO AND W. KLEIN, *J. Phys. A* **13** (1980), 2775.
110. D. STAUFFER, A. CONIGLIO, AND D. W. HEERMANN, *Phys. Rev. Lett.* **49** (1982), 1262.
111. For reviews, see J. D. GUNTON, M. SAN MIGUEL, AND P. S. SAHNI, *in* "Phase Transitions and Critical Phenomena" (C. Domb and J. L. Lebowitz, Eds.), Vol. 8, Academic Press, London, 1983; K. BINDER, *in* "Neutrons in Condensed Matter Research, Today and Tomorrow" (S. W. Lovesey and R. Scherm, Ed.), Plenum, New York, 1984.
112. B. WIDOM, *J. Chem. Phys.* **39** (1963), 2808; *J. Phys. Chem.* **86** (1982), 869.
113. D. J. ADAMS, *Mol. Phys.* **28** (175), 1241.
114. S. ROMANO AND K. SINGER, *Mol. Phys.* **37** (1979), 1765.
115. J. G. POWLES, *Mol. Phys.* **41** (1980), 715.
116. G. E. MURCH AND R. J. THORN, *Nucl. Metall.* **20** (1976), 245.
117. Z. ALEXANDROVICZ, *J. Stat. Phys.* **13** (1975), 231; **14** (1976), 1.
118. K. S. SHING AND K. E. GUBBINS, *Mol. Phys.* **46** (1982), 2109; **43** (1981), 717; K. K. MON AND R. B. GRIFFITHS, preprint.

119. J. G. POWLES, *Chem. Phys. Lett.* **26** (1982), 335; J. G. POWLES, W. A. B. EVANS, AND N. QUIRKE, *Mol. Phys.* **46** (1982), 1347.
120. J. A. ZOLLWEG, *J. Chem. Phys.* **72** (1980), 6712.
121. Z. W. SALSBURG, J. D. JACOBSEN, W. FICKETT, AND W. W. WOOD, *J. Chem. Phys.* **30** (1959), 65.
122. J. P. HANSEN AND L. VERLET, *Phys. Rev.* **184** (1969), 151.
123. K. BINDER, *J. Stat. Phys.* **24** (1981), 69.
124. K. BINDER, *Z. Phys. B* **45** (1981), 61.
125. T. L. POLGREEN, *Phys. Rev. B* **29** (1984), 1468.
126. S. K. MA, *J. Stat. Phys.* **26** (1981), 221.
127. S. K. MA AND M. PAYNE, *Phys. Rev. B* **24** (1981), 3984.
128. J. JÄCKLE AND W. KINZEL, *J. Phys. A* **16** (1983), L163.
129. Z. ALEXANDROWICZ, *J. Chem. Phys.* **55** (1971), 2765; H. MEIROVITCH AND Z. ALEXANDROWICZ, *J. Stat. Phys.* **16** (1977), 121; Z. ALEXANDROWICZ, *J. Stat. Phys.* **5** (1972), 19.
130. H. MEIROVITCH, *Chem. Phys. Lett.* **45** (1977), 389; *J. Stat. Phys.* **30** (1983), 681; *J. Phys. A* **16** (1983), 839; H. MEIROVITCH AND Z. ALEXANDROWICZ, *Mol. Phys.* **34** (1977), 1027.
131. H. MEIROVITCH, *Phys. Rev. B*, in press.
132. J. P. VALLEAU AND D. N. CARD, *J. Chem. Phys.* **57** (1972), 5457.
133. G. TORRIE AND J. P. VALLEAU, *Chem. Phys. Lett.* **28** (1974), 578; *J. Comput. Phys.* **23** (1977), 187; *J. Chem. Phys.* **66** (1977), 1402; see also [8] for a review.
134. G. E. MURCH, *in* "Diffusion in Solids II" (G. E. Murch and N. S. Nowick, Eds.), Academic Press, New York, in press.
135. M. BOWKER AND D. A. KING, *Surf. Sci.* **71** (1978), 583; G. E. MURCH AND R. J. THORN, *Philos. Mag.* **35** (1977), 493.
136. R. KUTNER, K. BINDER, AND K. W. KEHR, *Phys. Rev. B* **26** (1982), 2967; **28** (1983), 1846.
137. A. SADIQ AND K. BINDER, *Surf. Sci.* **128** (1983), 350.
138. K. W. KEHR, R. KUTNER, AND K. BINDER, *Phys. Rev. B* **23** (1981), 4931.
139. For a review, see A. BAUMGÄRTNER, *in* [28, Chap. 5].
140. G. CICOTTI, G. JACUCCI, AND I. R. MCDONALD, *J. Stat. Phys.* **21** (1979), 1.
141. M. Y. CHOI AND B. A. HUBERMAN, *Phys. Rev. B* **29** (1984), 2796.
142. J. F. SERINKO, in preparation.
143. H. J. HERRMANN, D. P. LANDAU, AND D. STAUFFER, *Phys. Rev. Lett.* **49** (1982), 412; H. J. HERRMANN, D. STAUFFER, AND D. P. LANDAU, *J. Phys. A* **16** (1983), 1221.
144. T. A. WITTEN AND L. M. SANDER, *Phys. Rev. Lett.* **47** (1981), 1400; P. A. MEAKIN, *Phys. Rev. A* **27** (1983), 604.
145. M. K. PHANI, J. L. LEBOWITZ, M. H. KALOS, AND O. PENROSE, *Phys. Rev. Lett.* **45** (1980), 366.
146. P. S. SAHNI, G. DEE, J. D. GUNTON, M. K. PHANI, J. L. LEBOWITZ, AND M. H. KALOS, *Phys. Rev. B* **24** (1981), 410.
147. P. S. SAHNI AND J. D. GUNTON, *Phys. Rev. Lett.* **47** (1981), 1754.
148. P. S. SAHNI, G. S. GREST, M. P. ANDERSON, AND D. J. SROLOWITZ, *Phys. Rev. Lett.* **50** (1983), 263; S. A. SAFRAN, P. S. SAHNI, AND G. S. GREST, *Phys. Rev. B* **28** (1983), 2693; P. S. SAHNI, D. J. SROLOVITZ, G. S. GREST, M. P. ANDERSON, AND S. A. SAFRAN, *Phys. Rev. B* **28** (1983), 2705; P. S. SAHNI, G. S. GREST, AND M. R. ANDERSON, *Phys. Rev. Lett.* **50** (1983), 60.
149. O. G. MOURITSEN, *Phys. Rev. B* **28** (1983), 3150, and preprint.
150. K. KASKI, M. C. YALABIK, J. D. GUNTON, AND P. S. SAHNI, *Phys. Rev. B* **28** (1983), 5263; K. KASKI, S. KUMAR, J. D. GUNTON, AND P. A. RIKVOLD, *Phys. Rev. B* **29** (1984), 4420.
151. A. SADIQ AND K. BINDER, *Phys. Rev. Lett.* **51** (1983), 674.
152. A. SADIQ AND K. BINDER, *J. Stat. Phys.* **35** (1984), 517.
153. G. S. GREST, D. J. SROLOVITZ, AND M. P. ANDERSON, *Phys. Rev. Lett.* **52** (1984), 1321.
154. D. STAUFFER, C. HARTZSTEIN, K. BINDER, AND A. AHARONY, *Z. Phys. B* **55** (1984), 325.
155. E. T. GAWLINSKI, K. KASKI, M. GRANT, AND J. D. GUNTON, preprint.
156. A. SADIQ, *Phys. Rev. B* **9** (1974), 2299.
157a. H. MÜLLER-KRUMBHAAR AND K. BINDER, *Int. J. Magn.* **3** (1972), 113.

157b. B. K. CHABRABARTY, H. G. BAUMGAERTEL, AND D. STAUFFER, *Z. Phys. B* **44** (1981), 333.
157c. S. MIYASHITA AND H. TAKANO, preprint.
158a. J. TOBOCHNIK, S. SARKER, AND R. CORDERY, *Phys. Rev. Lett.* **46** (1981), 1417; M. C. YALABIK AND J. D. GUNTON, *Phys. Rev. B* **25** (1982), 534; N. JAN, L. L. MOSELEY, AND D. STAUFFER, *J. Stat. Phys.* **33** (1983), 1.
158b. C. KALLE, Diploma thesis, University of Cologne, 1984, unpublished; and *J. Phys.* **A17** (1984), L801.
159. For reviews see K. BINDER AND D. STAUFFER, *in* [27, Chap. 8; 28, Chap. 8].
160. K. BINDER AND A. P. YOUNG, *Phys. Rev. B* **29** (1984), 2864.
161. A. J. BRAY, M. A. MOORE, AND P. REED, *J. Phys. C* **11** (1978), 1187.
162. R. OMARI, J. J. PRÉJEAN, AND J. SOULETIE, *J. Phys. (Paris)* **44** (1983), 1069.
163. R. FISCH AND A. B. HARRIS, *Phys. Rev. Lett.* **38** (1977), 785; these series are corrected and reanalyzed in F. BANTILAN AND R. G. PALMER, preprint.
164. I. MORGENSTERN AND K. BINDER, *Z. Phys. B* **39** (1980), 227.
165. R. N. BHATT AND A. P. YOUNG, preprint.